Earth-Science Reviews 237 (2023) 104293

Contents lists available at ScienceDirect

Earth-Science Reviews

journal homepage: www.elsevier.com/locate/earscirev

Quantitative analysis of aeolian stratigraphic architectures preserved in different tectonic settings

Grace I.E. Cosgrove [a,*], Luca Colombera [a,b], Nigel P. Mountney [a]

[a] School of Earth and Environment, Institute of Applied Geoscience, University of Leeds, Woodhouse, Leeds LS2 9JT, UK
[b] Dipartimento di Scienze della Terra e dell'Ambiente, Università di Pavia, Via Ferrata 1, 27100 Pavia, Italy

ARTICLE INFO

Keywords:
Dune
Subsidence
Basin
Foreland
Intracratonic
Rift

ABSTRACT

Despite a well-documented record of preserved sedimentary architectures of aeolian successions from a variety of different sedimentary basin types, relationships between tectonic setting and aeolian accumulation and preservation remain poorly constrained and largely unquantified. This study uses a database-informed approach to quantitatively document the variability in preserved sedimentary architecture of 56 globally distributed aeolian systems, and to relate these variations to differences in their basin settings. Three different tectonic settings are considered: intracratonic, foreland, and rift basins. Key finding are as follows. (1) Intracratonic basins are characterized by slow accommodation generation. They favour the accumulation and preservation of relatively thin aeolian genetic units; likely generated by dunes and interdunes that climbed at low angles, resulting in the accumulation and preservation of relatively thin dune and interdune elements. Depressed water tables – indicated by abundant dry interdune elements – left accumulated dune successions exposed above the erosional baseline, making them vulnerable to post-depositional reworking. This likely resulted in sporadic episodes of aeolian dune accumulation, between long episodes of sediment bypass or deflation, under conditions of low rates of net accommodation generation. (2) Rapid accommodation generation in the depocentres of foreland basins favours the preservation of thick dune-set and interdune elements, enabled by a rapid rate of rise of the accumulation surface that allowed bedform climb at relatively high angles. High rates of sediment supply associated with erosion of adjacent orogenic belts allowed the construction of large dunes. Elevated water tables – indicated by abundant wet interdune elements – may have allowed aeolian accumulations to be placed beneath the baseline of erosion shortly after deposition, thereby protecting them from potential post-depositional deflation. (3) Despite rift basins experiencing the highest rates of accommodation generation, their fills tend to be associated with the preservation of relatively thin dune and sandsheet elements. Elevated water tables, associated with rapid accommodation generation, create damp substrates and consequently restrict the availability of dry sand for dune construction. In the examples considered here, rapid accommodation generation outpaces sediment supply, favouring the construction and rapid migration of small dunes that consequently accumulate thin dune sets. Aeolian dunes in rift basins are also commonly reworked by fluvial and alluvial processes, in some cases likely related to orographic precipitation, associated with rift shoulder topography. Results of this analysis can be applied to improve predictions of the architecture of ancient aeolian successions at the basin scale, both in outcrop and in subsurface successions.

1. Introduction

1.1. Sedimentary Basins

A sedimentary basin is a depression that can accommodate sediments to a substantial thickness such that their accumulations may be preserved over geological timescales (Einsele, 2000; Miall, 2000; Leeder, 2011; Allen and Allen, 2013). Sedimentary basins can be differentiated based on their mechanisms of development and their subsidence histories (Xie and Heller, 2009; Allen and Allen, 2013; Fig. 1). Basins of the same type share commonalities: (1) similar formative mechanisms of basin development; (2) similar rates of accommodation generation; (3) similar basin lifespans – i.e. the duration of time during which the basin is actively evolving; (4) similar basin morphologies – i.e. the shape and

* Corresponding author.
E-mail address: g.i.e.cosgrove@leeds.ac.uk (G.I.E. Cosgrove).

https://doi.org/10.1016/j.earscirev.2022.104293
Received 15 August 2022; Received in revised form 18 November 2022; Accepted 16 December 2022
Available online 23 December 2022

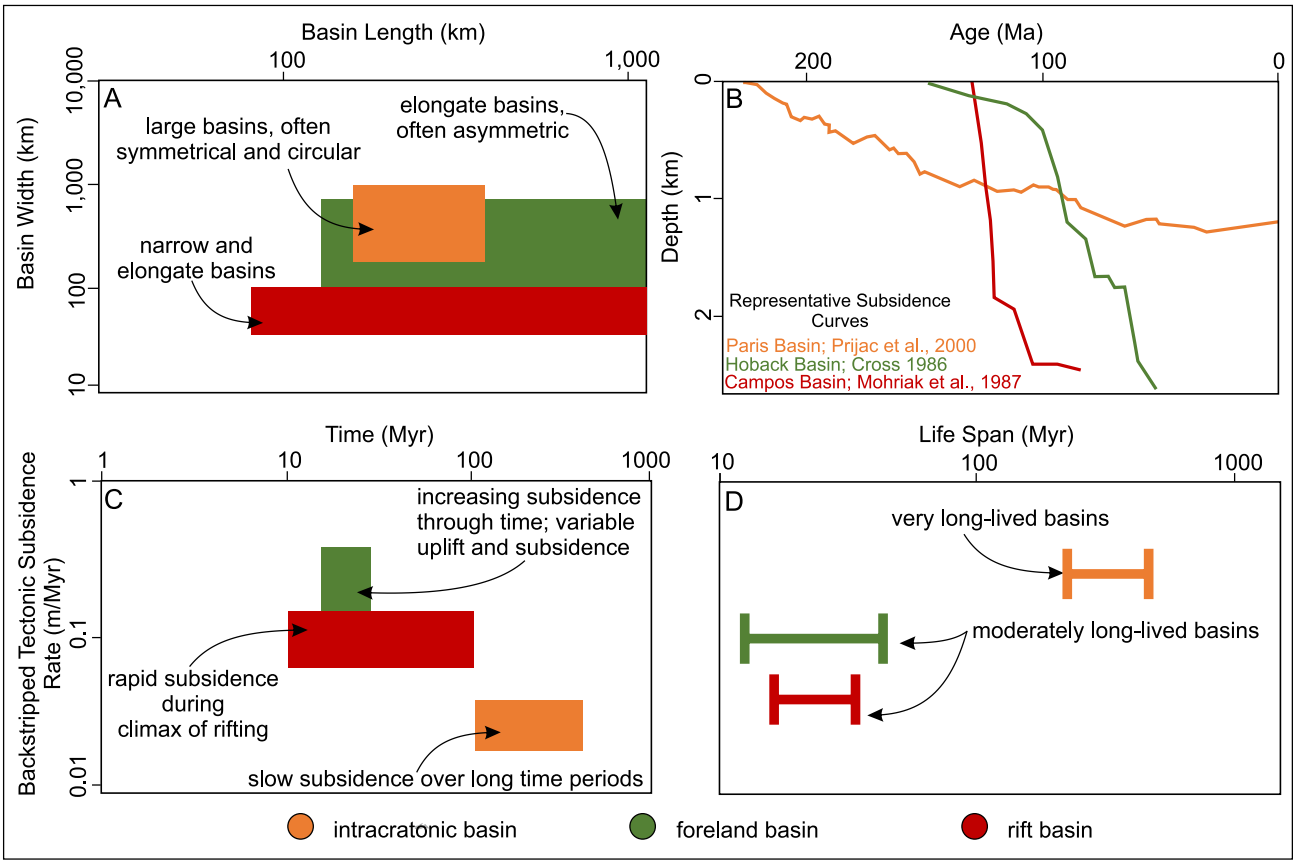

Fig. 1. A) Average basin widths and lengths according to basin type; B) representative tectonic subsidence curves according to basin type; C) average rates and duration of tectonic subsidence according to basin type; D) average basin duration according to basin type. Part D is modified after Woodcock (2004).

size of the basin; and (5) similar hinterland architectures – i.e. the structural evolution of the adjacent areas (Xie and Heller, 2009; Einsele, 2000; Allen and Allen, 2013; Fig. 1).

The interplay of tectonic basin-forming mechanisms and other extrinsic forcings – notably climate, the rate and type of sediment supply, and sea- or lake-level changes – ultimately determines the depositional environments that develop across a basin, and the manner in which sediments accumulate to form a basin infill (Mack, 1978). This study examines the nature of the preserved sedimentary record interpreted to have arisen in response to the operation of aeolian processes in three different tectonic settings: (1) intracratonic basins, (2) foreland basins, and (3) rift basins. The categorisation of case studies and their assignment to these three broad tectonic settings is based on the range of suitable data available in the published literature. Table 1 and Fig. 1 list and show summary descriptions of the main defining characteristics of these basin types.

1.2. Sedimentary accumulation in aeolian systems

Kocurek and Havholm (1993) define aeolian accumulation as 'net deposition through time such that a three-dimensional body of strata is formed' (p. 395). The subsidence of active sedimentary basins provides the most obvious mechanism for the generation of a large volume of space within which the long-term accumulation of aeolian deposits can occur. The sequestration of a sedimentary deposit into the geological record requires its placement beneath a baseline of erosion, such that it comes to lie within the available preservation space (Kocurek and Havholm, 1993; Howell and Mountney, 1997; Kocurek, 1999; Fig. 2A-D). In many circumstances, the level of the water table defines the erosional baseline. If the level of the water table remains static in absolute terms, gradual subsidence may still act to place an accumulating aeolian succession beneath this erosional baseline. Through this process, the long-term accumulation and preservation of aeolian deposits is enhanced; accumulated deposits lying beneath the level of the water table are protected to a large extent from post-depositional reworking and deflation (Kocurek and Havholm, 1993; Mountney, 2012; Fig. 2E).

Although examples of the preservation of the original topography and morphology of dunes are recorded in ancient successions (e.g. Clemmensen, 1988; Benan and Kocurek, 2000; Scotti and Veiga, 2019), they are not common. Instead, in the pre-Quaternary (i.e. "ancient") stratigraphic record, most aeolian deposits are represented by cross-stratified dune sets (Rubin and Hunter, 1982; Rubin, 1987; Kocurek et al., 1991). Dune sets most obviously form via the migration of dunes or megadunes (draa sensu McKee, 1979) over one another at low angles. During bedform climb, the migration of a succeeding bedform truncates the preceding bedform, thereby preserving only the lower portion of the original dune form as a set (Rubin and Hunter, 1982; Rubin, 1987; Kocurek et al., 1991). The ultimate thickness of dune sets preserved in the stratigraphic record is primarily a function of the size (i.e. the wavelength and height) of the original dunes and their angle of climb (Lancaster, 1985, 1992; Paola and Borgman, 1991; Kocurek and Havholm, 1993; Fig. 2F-I).

Despite attempts to understand the complex relationships between tectonics, the initial accumulation and the ultimate long-term preservation of aeolian sedimentary successions (e.g., Blakey, 1988; Blakey et al., 1988; Mountney et al., 1999; Scherer et al., 2007), the nature of the preserved aeolian record in relation to tectonic setting remains relatively understudied. Most previous studies on the relationship between aeolian architecture and basin type have consisted of largely qualitative accounts, and many are based on individual case studies (e.g. Clemmensen, 1987; Schenk et al., 1993; Basilici et al., 2009; Leleu and Hartley, 2010). The data presented in these individual case studies

Table 1
Summary of characteristics associated with the different basin types discussed in the text.

Basin Type	Basin Geometry	Formative Mechanism(s)	Subsidence Histories	Longevity of Basin	Nature of Basin Fill
Intracratonic Basins	Intracratonic (sag) basins are typically expressed as broad depressions – commonly large and circular in plan view (Fig. 1a) – in the interiors of cratonic blocks or on stable continental crust (Middleton, 1989).	Intracratonic basins form on the craton via differential subsidence relative to the neighbouring area of cratonic basement (Burgess, 2019). Subsidence occurs dominantly via simple thermal contraction without significant extensional faulting (Haxby et al., 1976; Klein and Hsui, 1987).	Intracratonic basins are characterized by relatively slow rates of accommodation generation (Einsele, 2000). Subsidence can be ongoing for many tens to hundreds of million years, yet may only cumulatively amount to one or two kilometres of tectonic subsidence over this time, though in some cases is more (Fig. 1b&c).	Intracratonic basins are very long-lived basins that record histories of accumulation over relatively long time spans (ca. 200–1000 Myr; Sloss and Speed, 1974; Sloss, 1988; Allen and Armitage, 2012; Einsele, 2000; Fig. 1d).	Mature intracratonic basins can host thick (ca. 10–15 km) and relatively undeformed sedimentary infills. The sedimentary fills of intracratonic basins may be subdivided into carbonate and terrigenous types. The former type is typically dominated by marine deposits with minor evaporites; the latter is dominated by continental clastic deposits, including aeolian and fluvial deposits, with limited or no marine shales (Selley and Sonnenberg, 2015)
Foreland Basins	Most foreland basins are characterized by a broadly asymmetric shape (Fig. 1a) with wedge-shaped profiles in section.	A foreland basin is a depression generated by flexure of the continental crust in front of a collisional fold-and-thrust mountain belt (Einsele, 2000). Foreland basins form due to loading by the mass generated by crustal thickening, associated with the evolution of a mountain belt in compressional settings.	Subsidence rates generally increase through time, but can be punctuated by episodes of uplift associated with thrust faulting and locally bulge migration (Fig. 1b & c). Subsidence histories reflect the rate of thrust development and propagation in the adjoining orogenic belt into the undeformed foreland, as compression continues. Subsidence of the foreland due to loading governs accommodation generation and determines the nature and rate of sedimentation in the basin (Einsele, 2000).	Foreland basins are relatively long-lived (ca. >10–70 Myr; Woodcock, 2004; Fig. 1d)	Foreland basins accumulate sediment eroded from the neighbouring mountain belt. Sedimentary successions are thickest adjacent to the mountain belt (the "foredeep") and thin away from the orogen. Typically, sedimentary facies are dominated by continental clastic deposits (fluvial, alluvial and aeolian) nearest to the adjacent mountain belt and pass laterally towards shallow- and deep-marine clastic deposits away from the mountain belt (Einsele, 2000).
Continental Rift Basins	Continental rift basins are relatively narrow and elongate (ca. 10^3–10^4 km^2) graben or half-graben troughs, or arrays of troughs, (Fig. 1a), bounded by normal faults (Einsele, 2000).	Rift basins are associated with active lithospheric extension and thinning (Gregory, 1894).	Initial phases of rifting are associated with rapid subsidence by faulting (e.g., Rosendahl, 1987; Schlische, 1993; Morley, 1995; Withjack et al., 2002). Subsequently, thermal contraction (re-equilibration) and sediment loading enables post-rift subsidence to continue (Fig. 1b & c).	Rift basins are relatively long-lived and their evolution typically spans from ca. >10–70 Myr (Woodcock, 2004; Fig. 1d).	Rift basins typically provide the greatest rates of accommodation generation of all basin types in terrestrial settings and are consequently associated with the accumulation of thick sedimentary infills and have long records of continental sedimentation (Einsele, 2000; Ashley and Renaut, 2002).

provide an opportunity to undertake a systematic study of potential relationships between tectonic setting and the aeolian sedimentary record. This is the focus of this work.

1.3. Aim and objectives

The aim of this study is to assess relationships between the tectonic setting and the resultant preserved sedimentary architectures of sand-dominated aeolian successions, interpreted as deposits of large-scale aeolian dune fields, ergs (sensu Wilson, 1973). Specific objectives are as follows: (1) to undertake a comprehensive quantitative analysis of the geometry, spatial relationships and lithological heterogeneity of aeolian successions developed in different basin settings; (2) to demonstrate the sedimentological variability seen in the studied aeolian successions; (3) to explain and discuss how preserved aeolian sedimentary architecture varies as a function of basin type and evolutionary history; (4) to present implications of the results for stratigraphic prediction and characterization, for example in subsurface settings.

To make meaningful comparisons between aeolian sedimentary deposits preserved in different basin types and settings, this study synthesizes quantitative sedimentological and stratigraphic data from 56 case studies of aeolian successions representing the infill of 37 different basins (Table 2). Data have been extracted from the published literature, and have been catalogued and analysed using a database-informed approach (see Cosgrove et al., 2021a). This study presents the first large-scale, global quantitative assessment of the relationship between the tectonic setting of sedimentary basins and aeolian sedimentary architectures. The case studies included in this investigation span geological time, from the Proterozoic to the Cenozoic, and are distributed globally (Fig. 3).

2. Methods

A relational-database approach is employed in this study (Cosgrove et al., 2021a; cf. Colombera et al., 2012, 2016). Data on the sedimentology of ancient aeolian case studies are stored in the Database of Aeolian Sedimentary Architecture (DASA; Cosgrove et al., 2021a, 2021b, 2022a, 2022b), which provides a record of the sedimentary architecture and organization of aeolian systems and their preserved succession. Data used in this study have been synthesized from 56 previously published case studies; each case study represents an ancient aeolian system (e.g., the Cedar Mesa Sandstone; Fig. 3; Table 2). In this investigation, case studies are grouped according to the type of basin in which they accumulated (Fig. 1; Tables 1 & 2).

Each case study considered in this analysis is associated with one or more sets of data (cf. 'subsets'; cf. Colombera et al., 2012). A subset

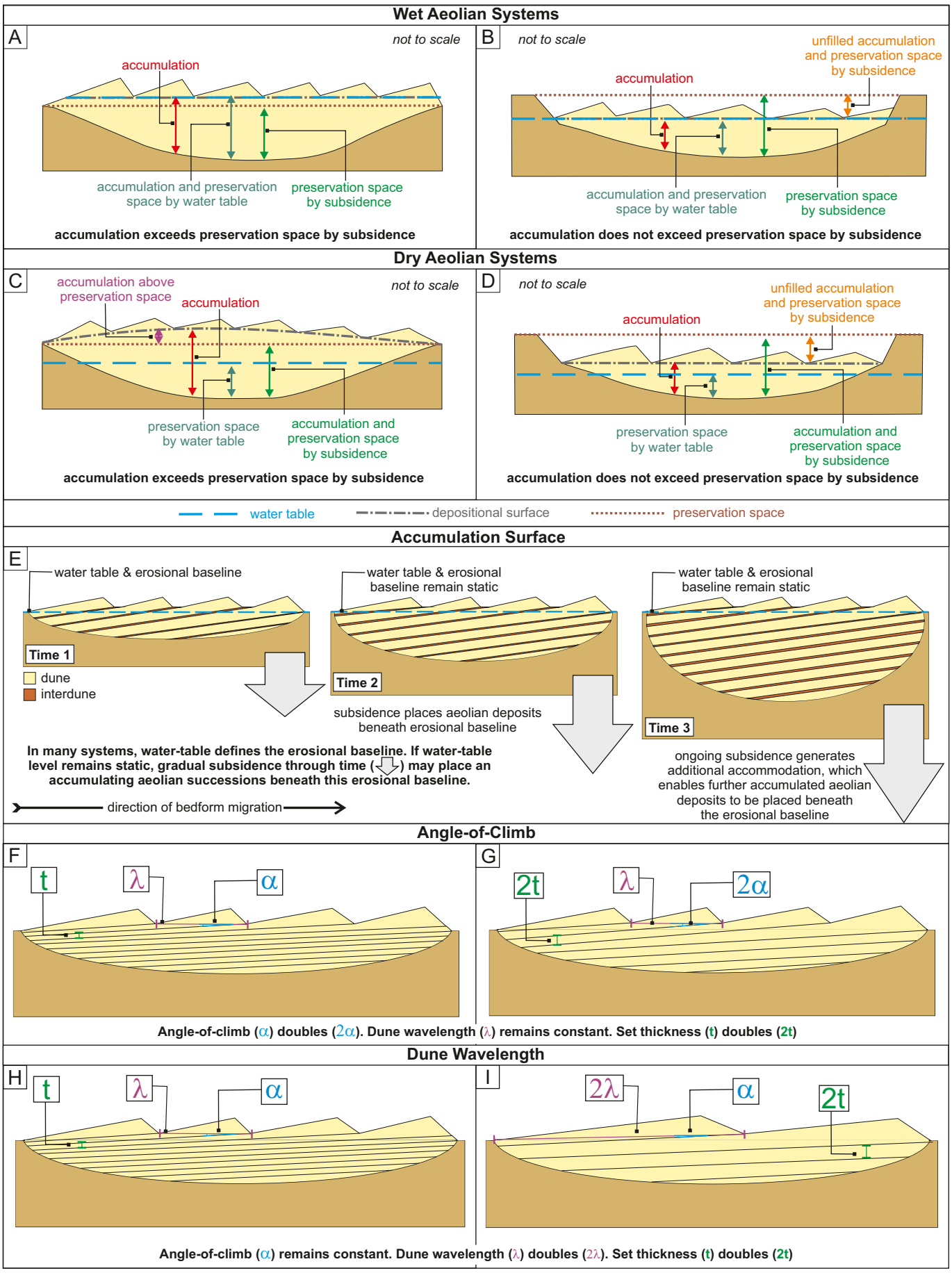

(caption on next page)

Fig. 2. Components of accumulation and preservation space for wet and dry aeolian systems. A) Wet aeolian system where water table rise has enabled the accumulation to build above the preservation space due to subsidence. A fall in water table will result in deflation. B) Wet aeolian system where the water table is below the preservation space line and the preservation space remains unfilled. C) Dry aeolian system where the accumulation has built above the preservation space because a positive net sediment budget exists. Long-term preservation potential of that part of the accumulation above the preservation space line is low. D) Dry aeolian system where the accumulation has not filled the available preservation space. Adapted in part from Kocurek and Havholm (1993). E) In many circumstances, the level of the water-table defines the erosional baseline. If the level of the water-table remains static, gradual subsidence may place accumulating aeolian successions beneath this erosional baseline. As such, the long-term accumulation and preservation of aeolian deposits is enhanced, as they are protected from post-depositional reworking and deflation. F-G) For dunes of a fixed wavelength, accumulated dune-set element thickness increases as the angle of climb increases. H—I) For dunes climbing at fixed angle of climb, accumulated dune-set element thickness increases as the dune wavelength increases.

signifies a collection of data (e.g., a sedimentary log or architectural panel) from an original data source (e.g., a publication or thesis). The types of data housed within each particular subset may vary considerably, depending on both the manner by which the original data were collected and in terms of the hierarchical levels they cover. Data standardization is undertaken upon data entry to DASA to ensure the use of consistent terminology and to reconcile the variety of source data types that were originally employed in the source literature to characterize the aeolian systems (see Cosgrove et al., 2021a for details).

DASA includes quantitative and qualitative data on geological entities of different types (e.g. architectural elements, lithofacies, textural properties, bounding surfaces), and on their depositional systems, themselves classified by multiple attributes (e.g., basin setting, aeolian physiographic setting, geological age) and metadata (e.g. data types, data sources). The case studies selected for inclusion in this investigation have been chosen to provide a broad global coverage of aeolian systems, which span age ranges from the Paleoproterozoic to the Cenozoic. For a full description of DASA, in terms of the database structure, database interrogation and database output and interpretation see Cosgrove et al. (2021a). All data used to generate the figures and tables presented in this article are provided in the Supplementary Information.

2.1. Scope of investigation

The potential importance of the basin setting on the resultant sedimentary architecture of aeolian systems has been interpreted from (1) comparisons of descriptive statistics by means of appropriate statistical tests, and (2) determination of correlation between variables. Quantitative data are supplemented by descriptive qualitative data, describing the sedimentary features associated with aeolian bodies that form architectural elements. In this context, architectural elements are bodies of strata with distinctive geometrical properties and composed internally of predictable associations of lithofacies, such that they can be interpreted in terms of the preserved record representative of components of aeolian systems (Cosgrove et al., 2021a; cf. Miall, 1985). In this investigation, output from DASA describes the following: (1) the relative proportion of architectural elements preserved in different basin settings; (2) the geometry of these sedimentary bodies; (3) the relationships between architectural-element lateral extent (i.e., length and width) and thickness; and (4) qualitative information relating to supersurfaces that delineate aeolian sedimentary sequences (sensu Fryberger, 1993; Kocurek, 1996). For definitions of all architectural element types and supersurface types discussed in the text, see Table 3.

2.2. Aeolian architectural element classifications

Architectural elements are discrete sedimentary units with specific sedimentological properties, including distinctive arrangements of internal facies units and bounding surfaces, and external geometries (cf. Miall, 1985). Several commonly occurring architectural element types, including dune, interdune and sandsheet elements, are routinely identified in aeolian successions (e.g., Kocurek, 1988; Karpeta, 1990). Architectural elements are the accumulated and preserved products of deposition in specific sub-environments (e.g. deposition in a dune, interdune or sandsheet setting). Architectural elements provide a record of both the vertical accumulation and lateral translation of accumulating components of the sedimentary system through time (cf. Mountney, 2012; Cosgrove et al., 2021a); as such, architectural elements have preserved geometries that do not necessarily resemble the form of the original components (e.g. a dune or an interdune); the environmental significance of an architectural element needs to be interpreted in the context of both its original geomorphic expression and its temporal evolution (Kocurek and Havholm, 1993). Non-aeolian architectural elements (e.g. elements of alluvial, fluvial or lacustrine origins) are recorded in DASA where they occur in association with aeolian-dominated deposits, for example, as in parts of the Jurassic Navajo Sandstone (Herries, 1993).

In the DASA framework used in this investigation, each individual recorded architectural element is assigned an interpretation that derives from the source literature (e.g. a dune set, interdune, sandsheet, or fluvial channel). Definitions of all architectural elements referred to in the main body of the text are defined in Table 3. In total, documented records of 3620 architectural elements have been examined (Fig. 4A), and their properties (external geometries and internal facies organization) have been quantitatively analysed.

2.3. Geometry and proportion of architectural elements and facies

For each architectural element, geometric properties (element thickness, length and width) are recorded, where such data are available. In this investigation, data on the thicknesses and lengths of architectural elements are considered in detail. Element lengths are recorded parallel to the overall inferred or reported direction of sediment transport. Reported thickness and length measurements are the maximum observable (or recorded) thickness or length of an architectural element, as presented in an outcrop panel, or graphic sedimentary log, for example. True, partial, and unlimited thicknesses and lengths are separately recorded (cf. Geehan and Underwood, 1993). The relative proportion of types of architectural and facies elements in successions, or in parts thereof, are considered as fractions of total recorded thicknesses. In all cases, the 'total recorded thickness' here refers only to the portions of a basin fill that are of aeolian or dominantly aeolian origin.

2.4. Bounding surfaces

The DASA framework used in this investigation has the capability to capture data relating to aeolian surfaces of all orders. Brookfield (1977) recognized a hierarchy of bounding surfaces (third-, second- and first-order). This scheme was augmented to assign descriptive identifiers of surface type by Kocurek (1996), who defined bounding-surface types of broadly equivalent significance to those of Brookfield (1977): reactivation surfaces, superposition surfaces, and interdune migration surfaces, respectively. A higher-order class of bounding surfaces is additionally now widely recognized: the supersurface (e.g., Loope, 1985; Langford and Chan, 1988; Fryberger, 1993; Kocurek, 1988, 1996). Reactivation, superposition and interdune surfaces are primarily the result of autogenic bedform migration, whereas supersurfaces are most commonly attributed as the product of allogenic forcing (e.g. Fryberger, 1993), though can also potentially be generated by the regional migration of a major aeolian sand-sea (or erg) system (e.g. Porter, 1986). In this investigation, due to their commonly large lateral extents and dominantly allogenic origin, only supersurfaces are considered in detail.

Table 2
List of the case studies used in this investigation; the 'Source Reference(s)' associated with each case study indicates the published literature source(s) from which data included in this investigation were derived. The geographic location of each case study is outlined in Fig. 3 (identified via the case number). Each case-study is associated with an average thickness, a duration of aeolian accumulation and rate of basin for subsidence for the time period specifically relating to aeolian accumulation; these values are derived from Cosgrove et al., 2022a. Case studies where accumulation rates have been used as proxies for subsidence rates are indicated by an asterisk.

Case Number	Case Study Name	Location	Basin Setting	Basin Name	Source Reference(s)	Average Thickness (m)	Duration of Aeolian Accumulation (Ma)	Basin Subsidence Rate (m/Myr)
1	Eriksfjord Formation	Greenland	Continental rift basin	Gardar Basin	Clemmensen (1988); Tirsgaard and Oxnevad (1998)	550	1	9.4*
2	Hopeman Sandstone	Scotland, UK	Foreland basin	Moray Firth Basin	Clemmensen (1987)	66	2	12.2
3	Arran Red Beds	Isle of Arran, Scotland, UK	Intracratonic basin	Mauchline Basin	Clemmensen and Abrahamsen (1983)	460	2	15.8
4	Sherwood Sandstone	UK (Onshore and Offshore England)	Continental rift basin	Cheshire Basin	Cowan (1993); Meadows and Beach (1993)	45	2	45.0
5	Rotliegendes Sandstone including Rotliegend Group	Germany, Poland, Denmark, Baltic Sea, Netherlands	Continental rift basin	NW German Basin	Ellis (1993); Newell (2001)	412	2	15.8
6	Boxtel Formation	Netherlands	Continental rift basin	Roer Valley Graben	Schokker and Koster (2004)	35	2	64.3
7	Sables de Fontainbleau Formation	France	Intracratonic basin	Paris Basin	Cojan and Thiry (1992)	60	2	19.5
8	Escorihuela Formation	NE Spain	Continental rift basin	Teruel Basin	Liesa et al. (2016)	33	1	2.6
9	Etjo Formation	Namibia	Intracratonic basin	Huab Basin	Mountney and Howell (2000)	200	3	168.0
10	Entrada Sandstone	Arizona, USA	Foreland basin	Paradox Basin	Kocurek and Day (2018)	300	2	26.4
11	Egalapenta Formation	India	Continental rift basin	Cuddapah Basin	Biswas (2005); Dasgupta et al. (2005)	400	1	5.7*
12	Tumblagooda Formation	Australia	Intracratonic basin	Carnarvon Basin	Trewin (1993)	731	2	31.0
13	Entrada Sandstone	New Mexico, USA	Foreland basin	Chama Basin	Benan and Kocurek (2000)	300	2	15.0
14	São Sebastião Formation	Brazil	Continental rift basin	Jatobá Basin	Ferronatto et al. (2019)	200	2	66.0
15	Sergi Formation	Brazil	Intracratonic basin	Recôncavo basin	Scherer et al. (2007)	450	3	100.5
16	Mangabeira Formation	Brazil	Intracratonic basin	São Francisco Craton	Bállico et al. (2017)	500	1	5.6*
17	Caldeirao Formation	Brazil	Intracratonic basin	Tucano Basin	Jones et al. (2016)	62	1	2.4*
18	Bandeirinha Formation	Brazil	Intracratonic basin	São Francisco Craton	Simplicio and Basilici (2015)	250	1	5.6*
19	Guara Formation	Brazil	Intracratonic basin	Paraná Basin	Scherer and Lavina (2005)	61	1	2.8
20	Piramboia Formation	Brazil	Intracratonic basin	Paraná Basin	Dias and Scherer (2008)	400	2	46.0
21	Cedar Mesa Sandstone	Colorado, USA	Foreland basin	Paradox Basin	Mountney and Jagger (2004)	200	2	11.9
22	Cedar Mesa Sandstone	Utah, USA	Foreland basin	Paradox Basin	Mountney (2006a)	200	2	13.0
23	Rio Negro Formation	Argentina	Intracratonic basin	Un-named basin	Zavala and Freije (2001)	50	2	15.3
24	Copper Habor Formation	Michigan, USA	Continental rift basin	Lake Superior Basin	Taylor and Middleton (1990)	1830	3	540.0
25	Chugwater Formation	Wyoming, USA	Intracratonic basin	Hanna Basin	Irmen and Vondra (2000)	300	2	11.4
26	Arikaree Formation	Wyoming, USA	Intracratonic basin	Denver Basin	Bart (1977)	100	1	8.3
27	Ingleside Formation	Colorado, Wyoming, USA	Intracratonic basin	Hanna Basin	Pike and Sweet (2018)	230	2	11.0
28	lower Cutler beds	Utah, USA	Foreland basin	Paradox Basin	Jordan and Mountney (2010); Wakefield and Mountney (2013)	200	1	9.1
29	Cedar Mesa Sandstone	Utah, USA	Foreland basin	Paradox Basin	Loope (1985)	442	2	33.5
30	Navajo Sandstone	Utah-Arizona border, USA	Foreland basin	Utah-Idaho Trough	Loope and Rowe (2003)	700	2	30.0
31	Entrada Sandstone	Utah, USA	Foreland basin	Utah-Idaho Trough	Crabaugh and Kocurek (1993)	300	2	21.3

(continued on next page)

Table 2 (*continued*)

Case Number	Case Study Name	Location	Basin Setting	Basin Name	Source Reference(s)	Average Thickness (m)	Duration of Aeolian Accumulation (Ma)	Basin Subsidence Rate (m/Myr)
32	Big Bear Formation	California, USA	Intracratonic basin	Southern Great Basin	Stewart (2005)	385	1	8.8*
33	Wolfville Formation	Nova Scotia, Canada	Continental rift basin	Fundy Basin	Leleu and Hartley (2018)	833	2	64.7
34	Page Sandstone	Utah, USA	Foreland basin	Utah-Idaho Trough	Jones and Blakey (1997)	56	2	61.6
35	Mancheral Quartzite	India	Continental rift basin	Cuddapah Basin	Chakraborty and Chaudhuri (1993)	50	2	13.3*
36	Venkatpur Sandstone	India	Continental rift basin	Cuddapah Basin	Chakraborty (1991)	70	2	13.3*
37	Unayzah A	Saudi Arabia	Continental rift basin	Greater Arabian Basin	Melvin et al. (2010)	30	1	2.7
38	Unayzah (middle member)	Saudi Arabia	Continental rift basin	Greater Arabian Basin	Melvin et al. (2010)	30	1	2.7
39	Karutola Formation	India	Continental rift basin	Central Indian Sandstone	Chakraborty and Sensarma (2008)	200	1	3.2*
40	Nepean Formation	Canada	Continental rift basin	Ottawa Basin	MacNaughton et al. (2002)	450	2	25.4
41	Pedra Pintada Formation	Brazil	Continental rift basin	Camaquã Basin	Paim and Scherer (2007)	120	2	10.9*
42	Whitworth Formation	Australia	Continental rift basin	McArthur Basin	Simpson and Eriksson (1993)	1325	2	54.6
43	Rodjeberg Formation	Greenland	Foreland basin	Danmarkshavn Basin	Olsen and Larsen (1993)	1100	2	98.0
44	Snehvide Formation	Greenland	Foreland basin	Danmarkshavn Basin	Olsen and Larsen (1993)	1100	2	98.0
45	Sofia Sund Formation	Greenland	Foreland basin	Danmarkshavn Basin	Olsen and Larsen (1993)	1100	3	145.5
46	Alinya Formation	Australia	Intracratonic basin	Officer Basin	Zang (1995)	750	2	51.0
47	Bakoye Formation	Africa	Intracratonic basin	Toudeni Basin	Deynoux et al. (1989)	125	1	5.0
48	Galesville Member	Wisconsin, USA	Intracratonic basin	Michigan Basin	Dott et al. (1986)	50	2	24.6
49	Kilmurry Formation	Ireland	Rift basin	Munster Basin	Morrisey et al. (2012)	1000	3	166.3
50	Lower Dala Sandstone	Sweden	Intracratonic basin	Sveconorwegian Basin	Pulvertaft (1985)	175	1	2.3*
51	Pewamo Formation	Michigan, USA	Intracratonic basin	Michigan Basin	Benison et al. (2011)	25	2	26.3
52	Shikaoda Formation	India	Intracratonic basin	Un-named basin	Chakraborty and Chakraborty (2001)	100	1	3.7*
53	St. Peter Sandstone	Wisconsin, USA	Intracratonic basin	Michigan Basin	Dott et al. (1986)	213	2	10.8
54	Wonewoc Formation	Wisconsin, USA	Intracratonic basin	Michigan Basin	Dott et al. (1986)	50	2	24.6
55	Varzinyha Formation	Brazil	Continental rift basin	Camaquã Basin	Paim and Scherer (2007)	200	2	10.9*
56	Page Sandstone	Arizona, USA	Foreland basin	Utah-Idaho Trough	Kocurek et al. (1991)	56	2	61.6

Supersurfaces record the boundaries of separate aeolian erg sequences, else record the transition of an aeolian accumulation to deposits of a different environmental type (Kocurek, 1988). To capture the stratigraphic significance of supersurfaces, a number of qualitative characteristics are recorded. First, the environmental significance of the supersurface is considered; namely, whether the supersurface is associated with a change in depositional environment, or an episode of bypass, or deflation (sensu Fryberger, 1993; Kocurek, 1996; Table 3). Second, sedimentary structures associated with a supersurface and which are indicative of the substrate conditions are considered (Table 3); these indicate whether the surface was associated with wet, damp, or dry surface conditions at the time of surface formation. Third, sedimentary structures indicative of surface stabilization are considered; these indicate whether the surface was stabilized or not prior to the onset of renewed sediment accumulation atop the surface (Ahlbrandt et al., 1978; Loope, 1988; Basilici et al., 2009; Dal'Bó et al., 2010; Krapovickas et al., 2016; Table 3). Definitions of all examined supersurface types are included in Table 3. In total, 190 supersurfaces have been analysed and 533 qualitative attributes associated with these supersurfaces have been measured. The vertical spacing (separation) of supersurfaces – i.e. the average thickness of genetic aeolian units – has been calculated by dividing the mean thickness of aeolian accumulations by the total number of supersurfaces in each basin setting.

2.5. Basin subsidence

Subsidence analysis is commonly undertaken in one-dimension, using data from measured stratigraphic sections and boreholes, from which the burial history of stratigraphic units can be reconstructed. For fuller descriptions of the methodologies associated with determining basin subsidence histories, refer to Allen and Allen (2013) and Lee et al. (2019). Rates of total basin subsidence collated from the literature, as presented in Cosgrove et al. (2022a), are recorded for each case study. In cases where there are no published subsidence curves for a particular basin, Cosgrove et al. (2022a) adopted sediment accumulation rates as proxies for total subsidence rates; twelve such cases are included in this study (Table 2). Subsidence rates reported here are not averaged for the entire time period of basin evolution, but only for the time period

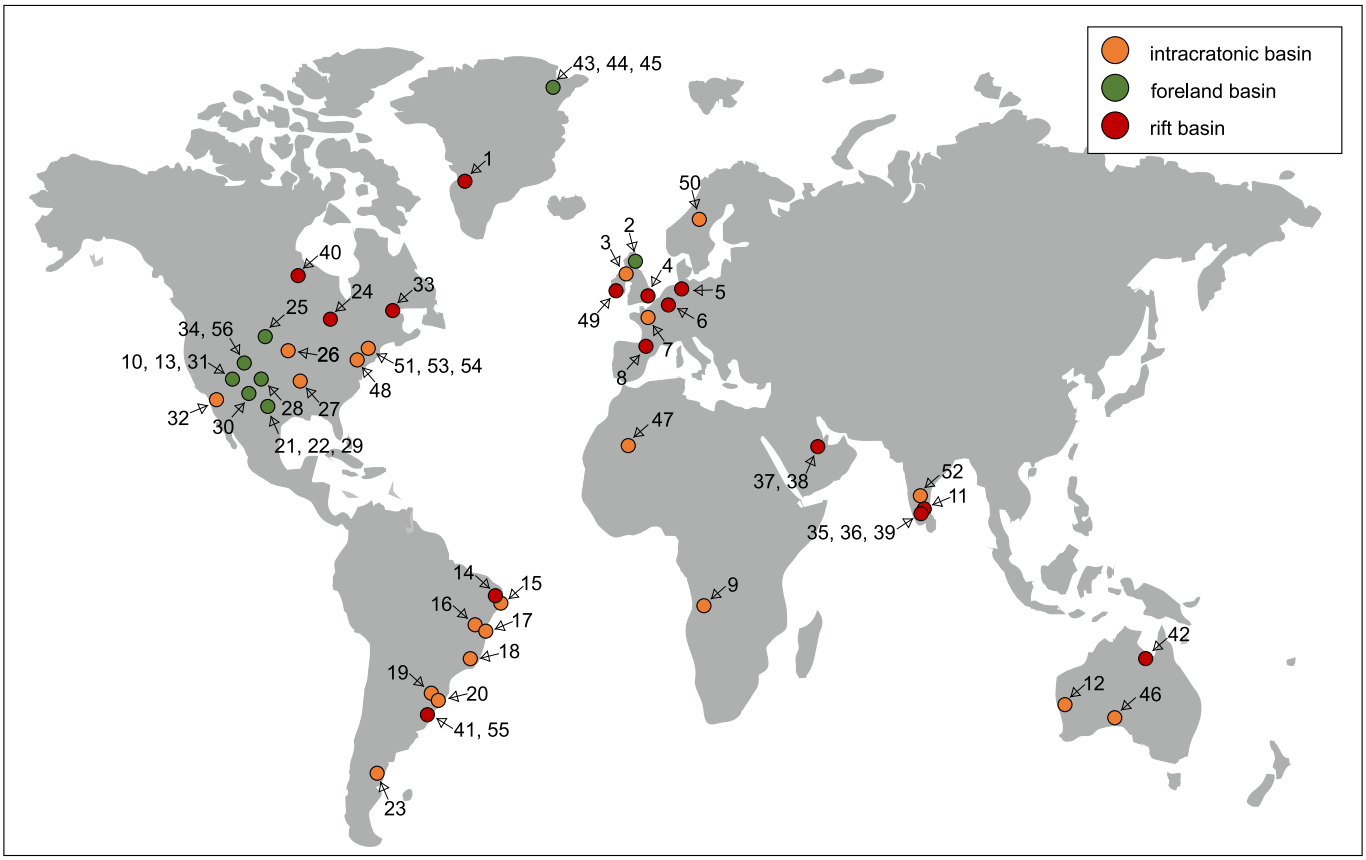

Fig. 3. World map showing the geographic distribution of 56 case-studies used in this investigation. Case studies are coloured according to basin type. The colours used in Fig. 1 to denote each basin type (i.e. orange = intracratonic basin; green = foreland basin; red = rift basin) are used throughout the figures in this study. (For interpretation of the references to colour in this figure legend, the reader is referred to the web version of this article.)

represented by aeolian-dominated accumulation.

2.6. Statistical analyses

Statistical analyses have been performed to reveal relationships between continuous variables (bivariate statistical analyses), and to test for significance in differences between the means of variables across groups (univariate statistical analyses). To quantify linear relationships between pairs of continuous variables that vary over orders of magnitude, the coefficient of determination (hereafter R^2) of power laws has been determined; the statistical significance of R^2 is expressed as a *P*-value (hereafter P).

For all univariate analyses, independent group ANOVA has been used to compare the means of more than two independent groups. Due to the non-normal and heteroscedastic distributions of architectural element thicknesses, independent group ANOVA was performed on log-transformed values of these variables (see Davis, 1986). The statistical significance of differences across groups are expressed as *P*-values (P). In all statistical analyses, P-values are compared with significance levels (α hereafter) that equals 0.05, to determine if the null hypothesis is rejected.

2.7. Limitations

There are a number of limitations associated with the methodology outlined here.

1. Absolute dating of ancient aeolian successions is challenging owing to the typical lack of datable materials (Rodríguez-López et al., 2014). In some instances, the presence of marine interbeds bearing macro- or micro-fossils, else the presence of extrusive volcanic deposits within otherwise aeolian-dominated aeolian successions, enables assignment to a biostratigraphic age or geochronometric dating (e.g. Jerram et al., 2000; Scherer, 2002; Petry et al., 2007).
2. It is common for aeolian successions to be partitioned internally by bounding surfaces (supersurfaces) that signify and document potentially long-lasting interruptions in accumulation (e.g., Loope, 1985; Mountney, 2006). In many instances, the aeolian accumulations themselves have been interpreted to represent significantly less time than the supersurfaces that bound and divide them; as such, a preserved aeolian succession may only represent a small fraction of the total geological time span over which the aeolian system was active (cf. Ager, 1976; Sadler, 1981; Loope, 1985). Due to geochronometric errors and the fragmentary nature of the aeolian record, the reported age ranges of aeolian deposits documented in the literature can be under- or over-estimates. As such, accumulation rates are time-dependent; this has implications when making comparisons between accumulation rates determined from different timescales (Cosgrove et al., 2022a).
3. Subsidence rates derived from the literature are themselves subject to error as a result of inaccuracies in the data used for the reconstruction of subsidence histories (see Xie and Heller, 2009).
4. In some instances, basin classifications (i.e. assignment of a case study to a specific basin type) may be contended. In these cases, the interpretation that is most widely supported in the recent scientific literature is considered.
5. The study relies on the interpretation of the palaeoenvironmental significance of aeolian architectural elements by the authors of the studies from which the data were sourced (i.e. the recognition of dune sets, interdunes and sandsheets). Full diagnostic criteria for the

Table 3
Definitions of aeolian and non-aeolian architectural elements and aeolian bounding surface types discussed in the text.

Aeolian Architectural Elements	
Dune Set	Dune sets form the fundamental unit of deposition of an aeolian sand dune; dune sets are formed of packages of cross-strata (Sorby, 1859; Allen, 1963; Rubin and Hunter, 1982; Chrintz and Clemmensen, 1993); if dunes migrate over each other, cross-stratified packages are truncated, delineating sets that are bounded by erosional surfaces (Brookfield, 1977; Kocurek, 1996).
Sandsheet	Sandsheet deposits are low-relief accumulations of aeolian sediment in areas where dunes are generally absent (Nielson and Kocurek, 1986); they can include low-relief bedforms such as zibars. Sandsheets rarely exceed 20 m in thickness and are typically preserved as tabular and laterally continuous sheet-like bodies.
Interdune	Interdune deposits are formed in the low-relief, flat, or gently sloping areas between dunes; neighbouring dunes are separated by interdunes; commonly referred to as the interdune corridors, interdune areas, or interdune hollows (Hummel and Kocurek, 1984). Interdunes architectural elements are preserved in a variety of shapes and styles; see below for detail.
Wet Interdune	Wet interdunes are characterized by deposits that accumulate on a substrate where the water table is elevated above the ground surface such that the interdune is episodically or continuously flooded with water (Kocurek and Havholm, 1993; Loope et al., 1995; García-Hidalgo et al., 2002). In cases where interdune flooding is caused by fluvial incursion, eet interdune architectural elements can reflect the immediate shape of the interdune pond or lake (Herries, 1993; Mountney and Jagger, 2004). Conversely, in cases where there is a sustained high water table but where dune migration is not curtailed – thick and laterally extensive wet interdune elements can accumulate to form laterally extensive and continuous wet interdunes.
Damp Interdune	Damp interdunes are characterized by deposits that accumulate on a substrate where the water table is at or close to the ground surface, such that sedimentation is influenced by the presence of moisture (Fryberger et al., 1988; Lancaster and Teller, 1988; Kocurek et al., 1991). Isolated damp interdunes with elliptical shapes ribbon-shaped architectural element as they translate through space over time. Conversely, laterally elongate interdune corridors that develop and migrate in front of straight-crested transverse dunes generate sheet-shaped architectural elements.
Dry Interdune	Dry interdunes are characterized by deposits that accumulate on a substrate where the water table is substantially below the ground surface, such that sedimentation is neither controlled nor greatly influenced by the effects of moisture (Fryberger et al., 1988). Resultant dry interdune architectural elements tend to be relatively thin and typically form only the lowermost metre or less of accumulated deposits above a bounding surface.
Non-Aeolian Architectural Elements	
Fluvial	Deposits arising from or relating to the action of streams and rivers.
Alluvial	Deposits arising from, or relating to the action of streams and sediment gravity-flow processes (cf. Melton, 1965).
Sabkha	Sabkhas and playa lakes are low-relief flats and shallow evaporitic lakes where evaporites, and in some cases carbonates, accumulate. The terms sabkha and playa lake were originally used to describe coastal and inland settings, respectively (Evans et al., 1964; Purser and Evans, 1973); however, the terms are now used interchangeably.
Marine	Deposits arising from or relating to the action of the sea.
Lacustrine	Deposits arising from or relating to accumulation in perennial lakes.
Igneous	Deposits relating to intrusive or extrusive volcanic activity.
Palaeosol	Preserved expression of ancient soils.
Surface Types	
Supersurface	Surfaces resulting from the cessation of aeolian accumulation; they occur where the sediment budget switches from positive to negative (cannibalization of aeolian system) or neutral (zero angle of climb), resulting in deflation (*deflationary supersurface*) or bypass (*bypass supersurface*) of the aeolian system, respectively. Supersurfaces are also generated by changes in depositional environment, such as transition from aeolian to fluvial, or aeolian to marine deposition (e.g., Glennie and Buller, 1983; Chan and Kocurek, 1988).
Wet-type supersurface	Supersurface associated with deflation down to the water-table (also known as a Stokes surface). Wet-type supersurfaces may be associated with aqueous inundation by a non-aeolian source (e.g., fluvial/marine deposits).
Damp-type supersurface	Supersurface associated with bypass/deflation; the level of the water table is interacting with the surface.
Dry-type supersurface	Supersurface associated with bypass/deflation; the level of the water table is significantly below the surface.

identification of aeolian architectural elements of different types are outlined in Table 2. To assign a measure of quality to interpretations, data added to DASA are classified in terms of perceived quality based on the type, quantity and resolution of the original source data (cf. Baas et al., 2005; Colombera et al., 2012, 2016). A threefold data quality index ('A', highest quality, to 'C', lowest quality) has been applied on the basis of expert judgement and quality criteria.

6. The number of architectural and lithofacies elements associated with a given case study is dependent on the original data source and is reflective of the type and scale of the original data source. It is well known that aeolian systems can exhibit complex lateral changes in architecture; for example, the aeolian-dominated Navajo Sandstone interdigitates both laterally and vertically with deposits of fluvial and sabkha origin in the adjoining Kayenta Formation over a spatial distance of ca. 75 km (Middleton and Blakey, 1983; Herries, 1993; Hassan et al., 2018). In such an example, the data collected from a regional stratigraphic architectural panel would differ from data presented in a 1D graphic sedimentary log depending on the position at which the log was recorded. To mitigate the effects of lateral aeolian system variability, this study utilizes a variety of data sources (including outcrop architectural and photo panels, cores, and well logs) to provide comprehensive, although not exhaustive, coverage of aeolian systems in all three basin types.

3. Results

The sedimentary architecture of aeolian-dominated successions forming the fills of sedimentary basins of different types are expected to differ, given that types of basins vary with respect to their subsidence histories, lifespans and tectonic configurations (Xie and Heller, 2009; Einsele, 2000; Allen and Allen, 2013). To assess the significance of these differences, aeolian sedimentary systems are grouped according to the tectonic setting of their basins: aeolian successions are grouped into the preserved deposits of intracratonic basins, foreland basins and rift basins. In DASA, aeolian systems from other tectonic settings (passive continental margins and back-arc basins) are also included; these are not considered in this study due to data paucity.

Results of statistical analyses are summarized in Tables 4 and 5, which outline the mean, median, standard deviation, number of observations and results of Independent Group ANOVA for variables of interest. The data used in all figures and statistical analyses are presented in the Supplementary Information.

3.1. Case study overview

Subsidence rates of the case studies analysed here have been grouped according to basin type; mean subsidence rates are 33.84 m/Myr, 47.86 m/Myr, and 58.55 m/Myr in intracratonic basins, foreland basins, and rift basins, respectively (Fig. 4B; Table 4). For each case study, a value of

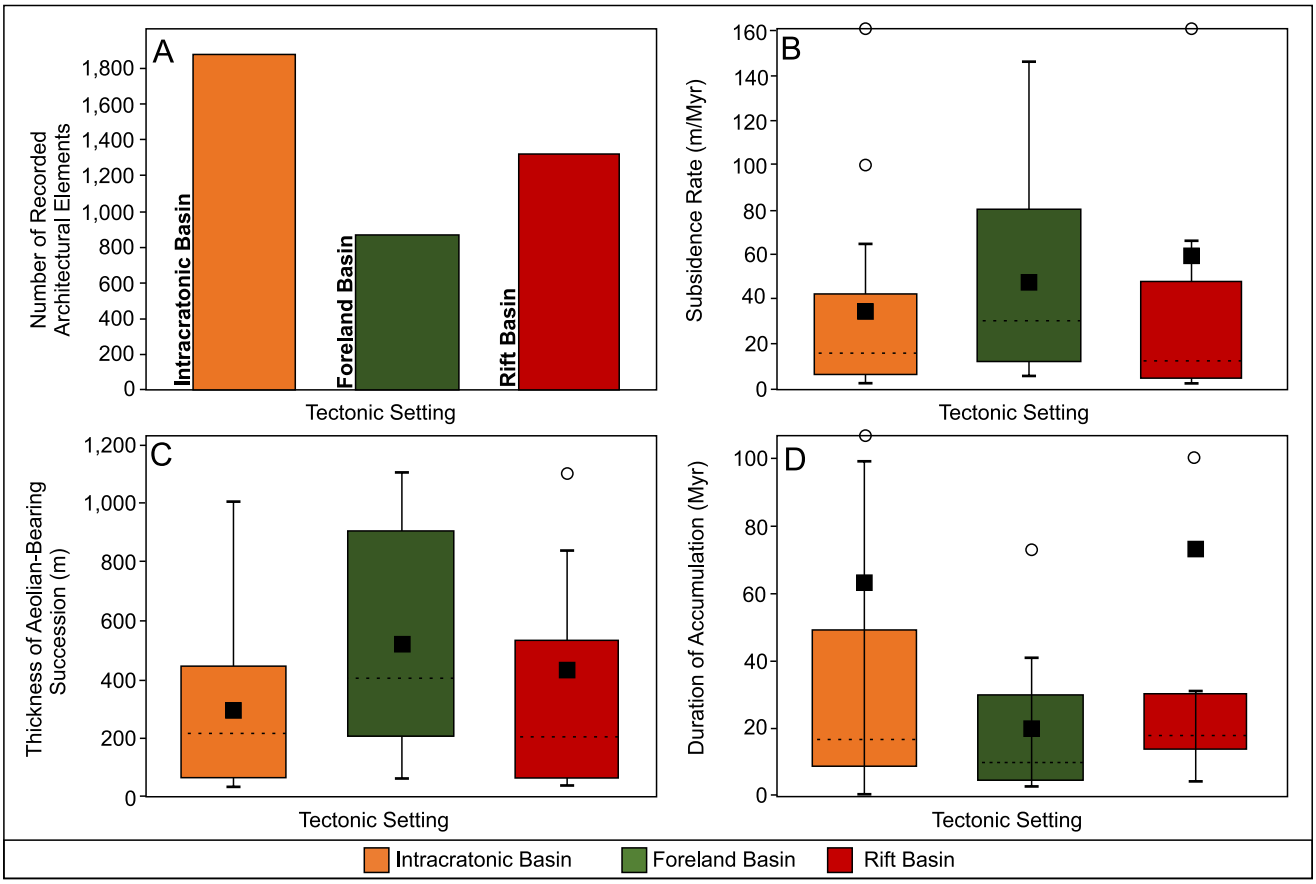

Fig. 4. A) Number of recorded architectural elements. B—D Box and whisker plots showing: B) average subsidence rate spanning the time-period of aeolian accumulation (m/Myr); C) average case study thickness of the aeolian accumulation (metres); D) average duration of aeolian accumulation (Myr). In all figures, data are grouped according to basin setting. Black square = mean; dashed line = median; white circle = outlier.

Table 4
Results of statistical analysis for rates of basin subsidence, case study thickness and the temporal duration of aeolian accumulation. All results are grouped according to basin setting.

	Intracratonic Basin	Foreland Basin	Continental Rift Basin
Basin Subsidence (m/Myr)			
N	26	11	14
Mean	33.8	47.9	58.6
Median	15.8	30.0	12.1
SD	45.4	46.7	140.5
ANOVA	>0.05		
Thickness of Aeolian-Bearing Succession (metres)			
N	26	11	14
Mean	293.2	514.9	422.9
Median	206.5	400	200
SD	272.3	416.8	550.8
ANOVA	>0.05		
Temporal Duration of Aeolian System (Myr)			
N	26	11	14
Mean	63.3	20.1	73.6
Median	17.0	10.0	18.0
SD	112.2	22.4	137.3
ANOVA	>0.05		

total thickness is determined as the total vertical extent of the studied aeolian stratigraphic succession, at its thickest position. The mean thickness of aeolian accumulations, including interbedded non-aeolian elements, is 293 m, 515 m and 423 m in intracratonic basins, foreland basins, and rift basins, respectively (Fig. 4C; Table 4). The mean temporal length of aeolian accumulation is 63.27 Myr, 20.09 Myr, and 73.64 Myr, for intracratonic basins, foreland basins, and rift basins, respectively (Fig. 4D; Table 4).

3.2. Architectural element assemblages

Ratios of proportions of aeolian to non-aeolian architectural elements are 63:37, 78:22, and 34:66 in intracratonic basins, foreland basins, and rift basins, respectively (Fig. 5A). Dune set elements form 81%, 90%, and 59% of the total aeolian stratigraphy, sandsheet elements form 15%, 8%, and 31% of stratigraphy, and interdune elements form 4%, 2%, and 10% of stratigraphy, in intracratonic basins, foreland basins, and rift basins, respectively (Fig. 5B).

In intracratonic basins, interdunes with sedimentary features indicative of dry (35%) and damp (35%) substrates form the greatest percentage of recorded interdune stratigraphy (Fig. 5C). In foreland basins, interdunes with sedimentary features indicative of wet (48%) substrates from the greatest percentage of recorded interdune stratigraphy (Fig. 5C). In rift basins, interdunes with sedimentary features indicative of damp substrates form the greatest percentage (45%) of recorded interdune stratigraphy (Fig. 5C).

When the interdigitating non-aeolian deposits are separately considered, in intracratonic basins, the most common non-aeolian elements are of fluvial (63%) and igneous (28%) origin (Fig. 5D). In foreland basins, the most common non-aeolian elements are of fluvial (39%) and sabkha (32%) origin (Fig. 5D). In rift basins, the most common non-aeolian elements are of fluvial (27%), alluvial (22%) and igneous (21%) origin (Fig. 5D).

Table 5
Results of statistical analysis for architectural element thickness and foreset dip. All results are grouped according to basin setting.

	Intracratonic Basin	Foreland Basin	Continental Rift Basin
All Aeolian Elements (metres)			
N	1095	536	665
Mean	4.7	4.4	2.2
Median	1.6	2.0	1.0
SD	8.7	6.5	3.4
ANOVA	P ≤0.01		
All Dune-Set Elements (metres)			
N	543	335	220
Mean	5.5	4.7	2.2
Median	2.0	2.5	1.3
SD	8.6	6.3	2.6
ANOVA	P ≤0.01		
All Sandsheet Elements (metres)			
N	168	76	200
Mean	3.3	1.7	1.3
Median	1.0	0.8	0.4
SD	10.9	3.4	2.6
ANOVA	P ≤0.01		
All Interdune Elements (metres)			
N	153	29	123
Mean	0.8	1.4	0.6
Median	0.3	0.5	0.3
SD	1.6	2.8	1.2
ANOVA	P ≤0.01		
All Non-Aeolian Elements (metres)			
N	556	224	493
Mean	4.8	2.2	3.5
Median	1.5	1.0	1.0
SD	12.0	4.2	8.1
ANOVA	*P* ≤0.05		
All Fluvial Architectural Elements (metres)			
N	438	145	212
Mean	3.0	1.3	2.1
Median	1.0	0.5	0.5
SD	4.8	1.7	4.6
ANOVA	P ≤0.01		
All Alluvial Elements (metres)			
N	5	–	61
Mean	0.3	–	5.6
Median	0.2	–	3.0
SD	0.3	–	9.0
ANOVA	P ≤0.01		
All Sabkha and Playa Lake Elements (metres)			
N	4	34	34
Mean	2.6	4.5	2.7
Median	2.0	2.6	2.5
SD	1.7	6.6	2.1
ANOVA	P ≥0.05		
All Marine Elements (metres)			
N	33	33	89
Mean	3.3	2.1	3.0
Median	3.0	2.0	1.0
SD	2.7	1.2	5.4
ANOVA	P ≤0.05		
All Lacustrine Elements (metres)			
N	45	6	14
Mean	1.6	11.4	5.6
Median	1.0	4.0	5.0
SD	1.7	15.2	3.1
ANOVA	P ≤0.01		
All Igneous Elements (metres)			
N	12	–	14
Mean	48.4	–	24.2
Median	44.8	–	20.0
SD	42.0	-	20.1
ANOVA	P ≥0.05		
All Palaeosol Elements (metres)			
N	8	5	39
Mean	1.7	0.7	1.1
Median	0.8	0.5	0.8
SD	3.0	0.3	0.9
ANOVA	P ≥0.05		
Dune Foreset Dip (Degrees)			
N	41	23	26
Mean	27.4	21.9	19.5
Median	22.0	21.9	26.0
SD	17.5	<0.01	10.9
ANOVA	P ≥0.05		

Considering internal dune-set facies architecture, interfingered wind-ripple, grainfall and grainflow strata form 41%, 42%, and 57% of recorded dune-set facies types in intracratonic, foreland, and rift basins, respectively. Interfingered grainflow and grainfall strata form 33%, 46% and 35% of recorded dune-set facies types in intracratonic, foreland and rift basins, respectively. (Fig. 5E).

3.3. Architectural element thicknesses

Summary statistics on the thicknesses of all architectural elements are presented in Table 5 and thickness data are graphically presented in Fig. 6. Notably, there is a statistically significant difference ($P \leq 0.01$; Table 5) between basin types in the mean of log-transformed values of thickness of: (1) aeolian dune set elements (Fig. 6B); (2) sandsheet elements (Fig. 6C); (3) interdune elements (Fig. 6D); and (4) non-aeolian elements (Fig. 6E), between groups.

The largest median aeolian dune-set thicknesses are recorded in foreland basins; the thinnest are recorded in rift basins (Table 5; Fig. 6B). The thickest median aeolian sandsheet elements are recorded in intracratonic basins; the thinnest are recorded in rift basins (Table 5; Fig. 6C). The thickest median interdune elements are recorded in foreland basins; the thinnest are recorded in rift basins (Table 5; Fig. 6D).

3.4. Supersurfaces

Summary information relating to classes of supersurfaces is provided in Table 6 and Fig. 8. Based on supersurface classifications of Fryberger (1993) and Kocurek (1996), the following results are noted. Bypass supersurfaces are recorded most often in intracratonic basins (11%; Fig. 8A); deflation supersurfaces are recorded most often in foreland basins (74%; Fig. 8B); supersurfaces indicative of a change in depositional environment are recorded most often in intracratonic basins (47%; Fig. 8A). Supersurfaces associated with sedimentary structures indicative of wet substrate conditions are recorded most often in rift basins (90%; Fig. 8F); supersurfaces with sedimentary structures indicative of damp substrate conditions are recorded most often in foreland basins (16%; Fig. 8E); supersurfaces with sedimentary structures indicative of dry substrate conditions are recorded most often in intracratonic basins (15%; Fig. 8D). Supersurfaces associated with sedimentary structures indicative of stabilized conditions are recorded most often in foreland basins (43%; Fig. 8H); supersurfaces with sedimentary structures indicative of unstabilized conditions are recorded most often in rift

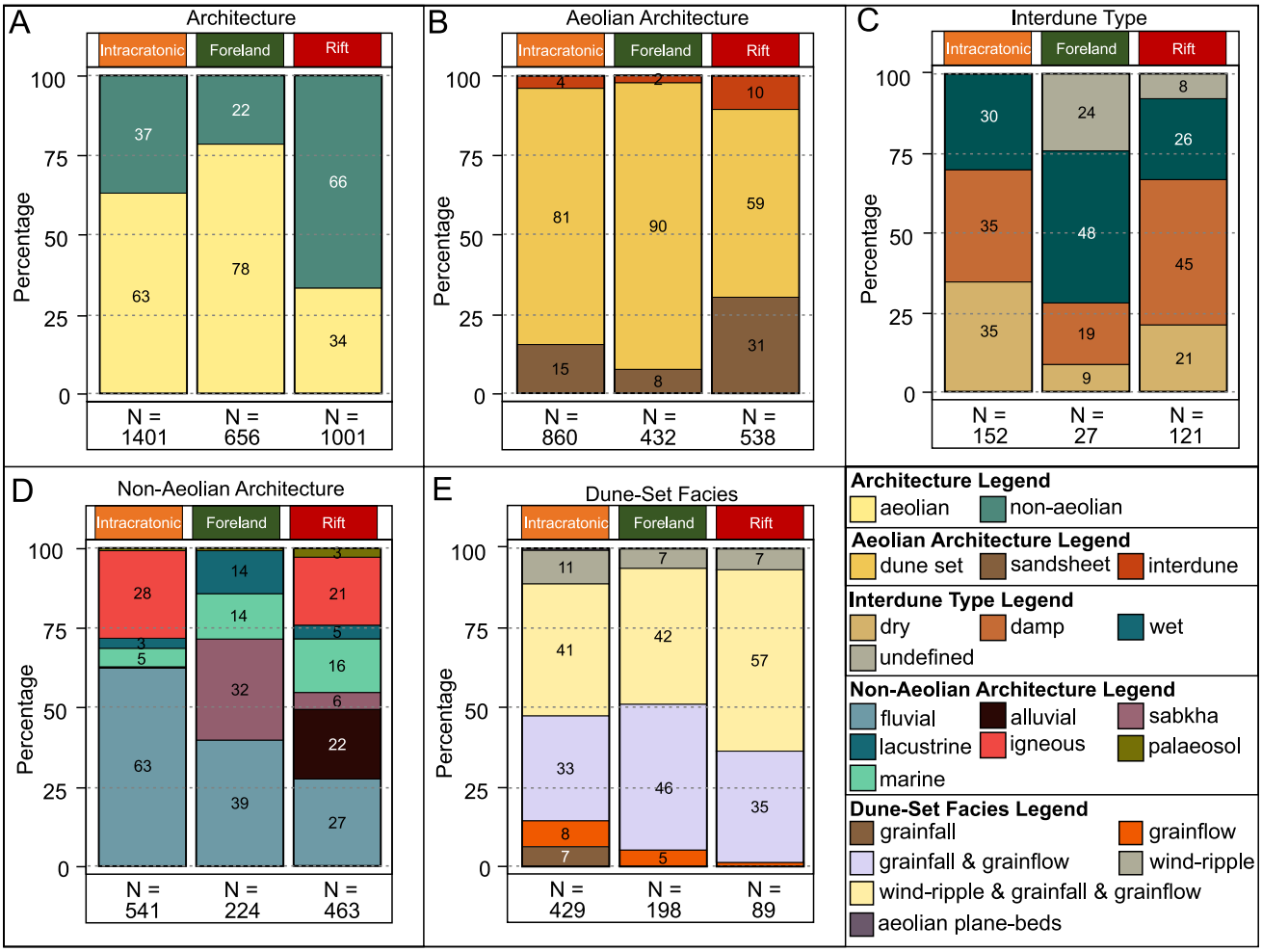

Fig. 5. A) Proportion of aeolian and interdigitating non-aeolian elements; B) proportion of aeolian element (dune-set, interdune and sandsheets) types; C) proportion of interdune element types (dry, damp, wet and undifferentiated; sensu Kocurek, 1981, Mountney, 2006); D) proportion of non-aeolian element types; E) proportion of facies types found in dune-set elements. All percentages are determined based on the total recorded lithology. All data are subdivided according to basin setting.

basins (100%; Fig. 8I). Average supersurface spacing – i.e. the thickness of aeolian genetic units – is 7.4 m, 11.9 m, and 20.1 m in intracratonic, foreland and rift basins, respectively.

3.5. Architectural element length and thickness

Relationships between aeolian architectural element length and thickness are considered (i.e. for dune set, sandsheet and interdune elements). In intracratonic basins, there is a weak ($R^2 = 0.37$) but statistically significant ($P \leq 0.01$) positive relationship between aeolian architectural element length and thickness (Fig. 7A). In foreland basins, there is no relationship between aeolian architectural element length and thickness ($R^2 = 0.10$; Fig. 7B). In rift basins, there is a statistically significant positive relationship ($R^2 = 0.67$; $P \leq 0.01$) between aeolian architectural element length and thickness (Fig. 7C).

3.6. Dune foreset dip

Dune foresets dip (at the angle of repose) at median values of 22.0°, 21.9°, and 26.0°, in intracratonic, foreland, and rift basins, respectively. Measured angles are corrected to remove any effects of tectonic tilting; however, the reported values are not corrected for sediment compaction.

4. Discussion

The sedimentary architectures of aeolian successions are governed by complex interactions between tectonic basin-forming mechanisms, and other extrinsic forcings, notably climate, sea level, sediment supply, and rates of change thereof (Blakey et al., 1988; Clemmensen et al., 1994; Cosgrove et al., 2021b, 2022b). These forcing mechanisms affect the behaviour of aeolian systems in a variety of ways. They influence: (1) the regional angle of climb of aeolian dune and interdune elements (e.g., Kocurek and Havholm, 1993; Mountney and Howell, 2000); (2) the size of the formative dunes (wavelength; Mountney, 2012); (3) relative and absolute changes in the level of the water table (Kocurek et al., 2001); (4) the presence of vegetation and other stabilizing agents (Gibling and Davies, 2012; Santos et al., 2017, 2019); (5) the rate and type of sediment supply (Kocurek and Lancaster, 1999); and (6) interactions with contiguous non-aeolian depositional environments (Chakraborty and Chaudhuri, 1993; Ferronatto et al., 2019). These influences on aeolian architectures and basin fills are discussed below in relation to tectonic setting.

4.1. Angle of climb and dune wavelength

The relative thickness of aeolian dune-set and interdune elements is, in part, controlled by a combination of the size of the formative dunes and their angle of climb (Fig. 2).

In almost all cases, rates of lateral dune migration greatly exceed

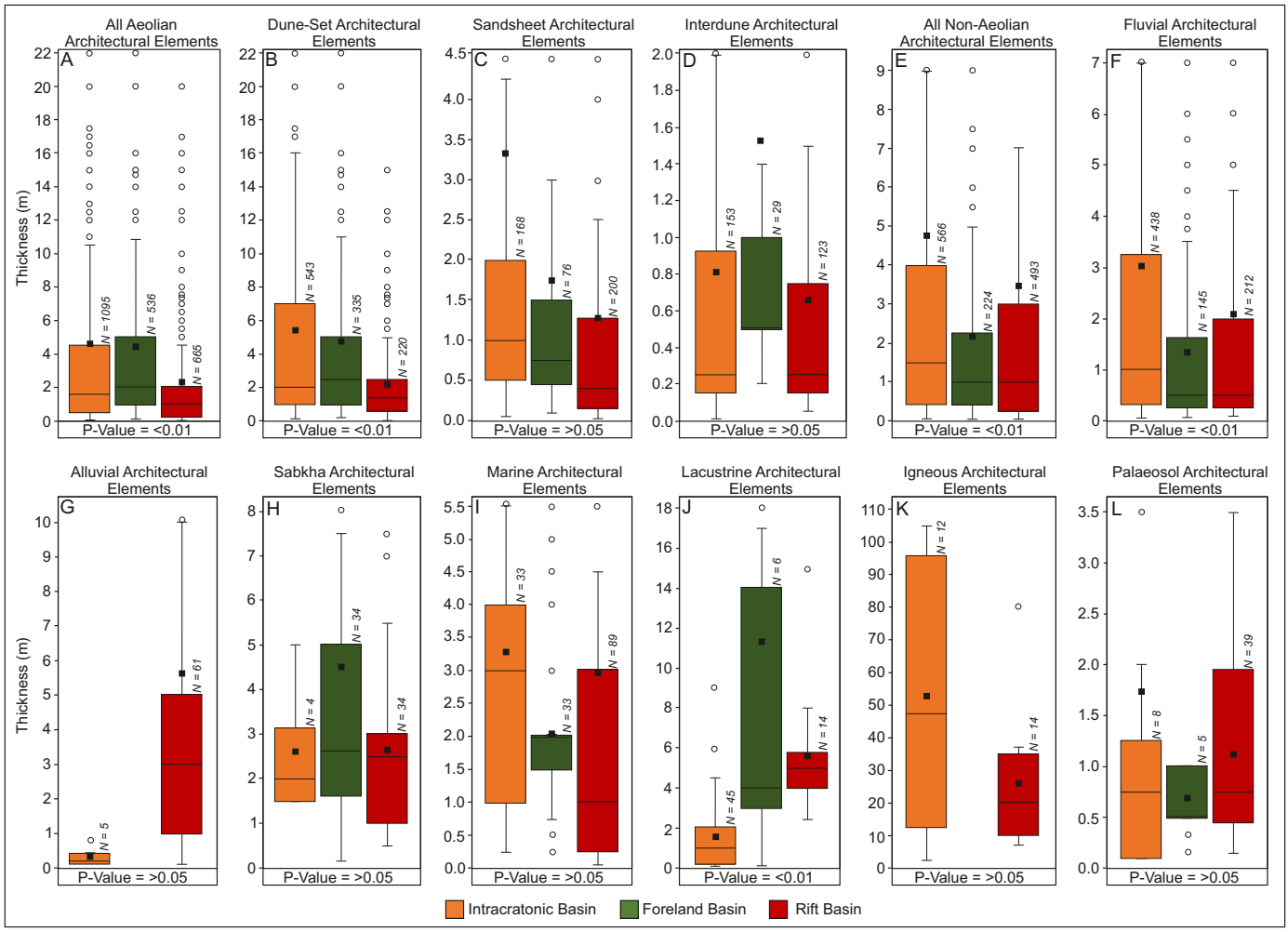

Fig. 6. Box and whisker plots showing thicknesses of A) all aeolian elements, B) dune-set elements, C) sandsheet elements, D) interdune elements, E) all non-aeolian elements, F) fluvial elements, G) alluvial elements, H) sabkha elements; I) marine elements; J) lacustrine elements; K) igneous elements, L) palaeosol elements. All data are subdivided according to basin type. For definitions of all architectural element types, refer to Table 3. Black square = mean; dashed line = median; white circle = outlier.

Table 6
Summary of supersurface characteristics. All results are grouped according to basin setting.

	Supersurface Classification (sensu Fryberger, 1993 and Kocurek, 1996) (percent)			Sedimentary structures indicative of substrate conditions (percent)			Sedimentary structures indicative of surface stabilization (percent)		Supersurface spacing; i.e. genetic unit thickness (metres)
	Bypass	Deflation	Environmental Change	Wet	Damp	Dry	Stabilized	Unstabilized	
Intracratonic Basins	11	42	47	73	12	15	8	92	7.4
Foreland Basins	0	74	26	74	16	10	43	57	11.9
Continental Rift Basins	6	68	26	90	5	5	0	100	20.1

time-averaged rates of basin subsidence, even where large bedforms migrate relatively slowly. As such, measured angles of bedform climb in aeolian successions are typically rather low. For example, the measured angle of bedform climb in part of the Jurassic Entrada Sandstone of eastern Utah is 0.09° (Gross et al., 2022). The angle of climb in of part of the Permian Cedar Mesa Sandstone in southern Utah varies from 0.3° to 0.7° (Mountney, 2006). Only rarely (and typically only for exceptional reasons) do measured angles of bedform climb exceed 1°, as is the case for part of the Cretaceous Etjo formation (now the Twyfelfontein Formation) in northern Namibia, where the migration of a large bedform to fill a pre-existing topographic hollow resulted in a localised angle of climb of 4.7° (Mountney and Howell, 2000).

Considering the angle of climb, rapid rates of subsidence and accommodation generation likely enable a faster rate of rise of the level of the accumulation surface, which allows bedforms to climb at angles that are relatively steeper (though typically angles of climb are still small and are only of a few tenths of a degree for a given rate of bedform migration). Consequently, relatively less of the underlying bedform is truncated, leading to the preservation of relatively thicker dune-set and interdune elements, and a greater proportion of the original landforms (Kocurek and Havholm, 1993; George and Berry, 1997; Howell and Mountney, 1997; Cosgrove et al., 2022a). Conversely, under slow rates

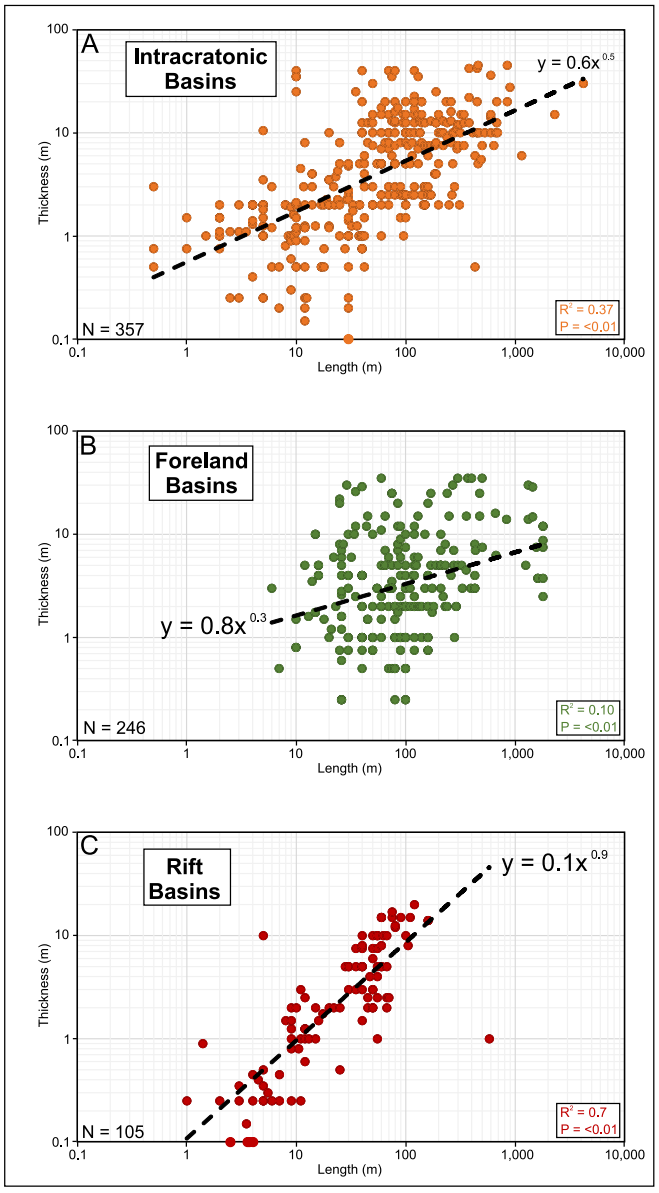

Fig. 7. Relationship between aeolian element thickness and length for: A) intracratonic basins, B) foreland basins, and C) rift basins.

of subsidence and accommodation generation, a slower rate of rise in the level of the accumulation surface limits bedform climbing to very low angles: relatively more of the underlying bedform is truncated (Fig. 2). In many cases, episodic aeolian accumulation may only be enabled in the immediate aftermath of episodes where accommodation is generated, for example following punctuated fault movements.

The original size (wavelength) of the dunes is a function of the availability of sediment for aeolian dune construction, the transport capacity of the wind, and its flow behaviour (Lancaster, 1985; Lancaster, 1992; Kocurek and Lancaster, 1999). The migration of dunes with larger wavelengths might potentially lead to the accumulation of thicker dune-set elements (Fig. 2), though not in all cases. The wavelength of the original dunes may also influence the angle of climb, because larger dunes tend to migrate at a slower rate than smaller dunes (Werner, 1995; Gay, 1999). As such, larger dunes may be associated with steeper angles of climb because the ratio between the rates of aggradation and dune migration tends to be higher (Mountney and Thompson, 2002; Mountney, 2006; Mountney, 2012). However, larger and more slowly migrating dunes tend to develop in the centres of large dune fields, many modern examples of which are present in the central parts of stable cratons that typically experience slow rates of subsidence (e.g., Saharan Metacraton; Abdelsalam et al., 2002) and the Arabian Nubian-Shield (Johnson and Woldehaimanot, 2003). In this context, despite the slow migration rates associated with long-wavelength dunes, the limited rate of accommodation generation may still result in the preservation of relatively thin dune-set elements and thin aeolian genetic units (Table 6; Mountney and Thompson, 2002; Mountney, 2006, 2012).

When the aeolian-dominated infills of foreland basins are considered, dune-set and interdune elements have the highest recorded median thickness of other basin type (Fig. 6B, D). Foreland basins record the second highest mean rate of subsidence among the studied examples (Fig. 4B): the associated rapid accommodation generation likely caused the relatively high angles of bedform climb, associated with rapid rises in the level of the accumulation surface (Kocurek and Havholm, 1993; George and Berry, 1997; Howell and Mountney, 1997; Cosgrove et al., 2022a). Additionally, the potential for the generation of large dune forms may partly relate to the physiography of foreland basins, whereby uplifting orogenic mountain belts bordering these basins are subject to relatively high rates of denudation (e.g., Mascle and Puigdefabregas, 1998) generating abundant sediment supply for the construction of large dunes. Foreland basins provide the conditions required to facilitate both relatively high angles of climb and the generation of relatively large formative dunes; both of these factors may contribute to the preservation of thick dune-set and interdune elements in the fills of foreland basins.

Subsidence rates determined for the aeolian-dominated portions of intracratonic basin fills tend to be lower on average than those recorded in foreland and rift basins (Fig. 4B). The subsidence histories of intracratonic basins typically reflect thermal subsidence of an initially thick continental lithosphere (Nunn and Sleep, 1984; Stel et al., 1993; Xie and Heller, 2009), commonly on ancient stable cratons. The relatively slow generation of accommodation in intracratonic basins may favour the accumulation and preservation of relatively thin aeolian dune-set and interdune elements (Table 6), and aeolian dune climb at low angles.

Rift basins are associated with the highest mean rates of subsidence (Fig. 4B); such high rates of accommodation creation should intuitively translate to relatively high angles of bedform climb and the generation of thicker aeolian dune-set elements (Kocurek and Havholm, 1993; George and Berry, 1997; Howell and Mountney, 1997; Cosgrove et al., 2022a). However, dune-set elements are thinner in rift basins than in any other basin setting (Fig. 6A-D). Given that the thicknesses of accumulated aeolian dune set elements is determined by the relationship between the angle of climb *and* the size of the original formative dunes, it can be inferred that dune-set thicknesses in rift basins considered here may be limited by the sizes of the formative dunes, though might additionally be influenced by the rate of migration of those dunes (Kocurek, 1999; Mountney and Howell, 2000).

Considering the modern aeolian sedimentary record, a compilation of the main Quaternary (modern) inland dune fields presented in Rodríguez-López et al. (2014) indicates that crescentic (barchan) dunes are the most common geomorphic dune type on Earth and Mars. Alongside ubiquitous crescentic dunes: (1) dunes developed in rift-basin settings are more likely to be of parabolic types; (2) dunes developed in foreland and intracratonic basins are more likely to be of linear types. Crescentic forms are typically the smallest type of dune, attaining maximum lengths, widths and heights of 0.1 km, 0.1 km and 0.01 km, respectively (Pye and Tsoar, 2008). Although crescentic dunes are common to all basin settings, linear dunes (preferentially found in intracratonic and foreland basins) tend to be larger in size that their parabolic dune (preferentially found in rift basins) counterparts. Linear dunes are known to attend maximum lengths, widths and heights of >100 km, 2 km, and 0.4 km, respectively (e.g. Breed and Grow, 1979; El-Baz et al., 1979; Lancaster, 1985). Conversely, parabolic dunes attain maximum lengths, widths and heights of 2.6 km, 2.4 km and 0.3 km, respectively (Breed and Grow, 1979). As such, the distribution of dune

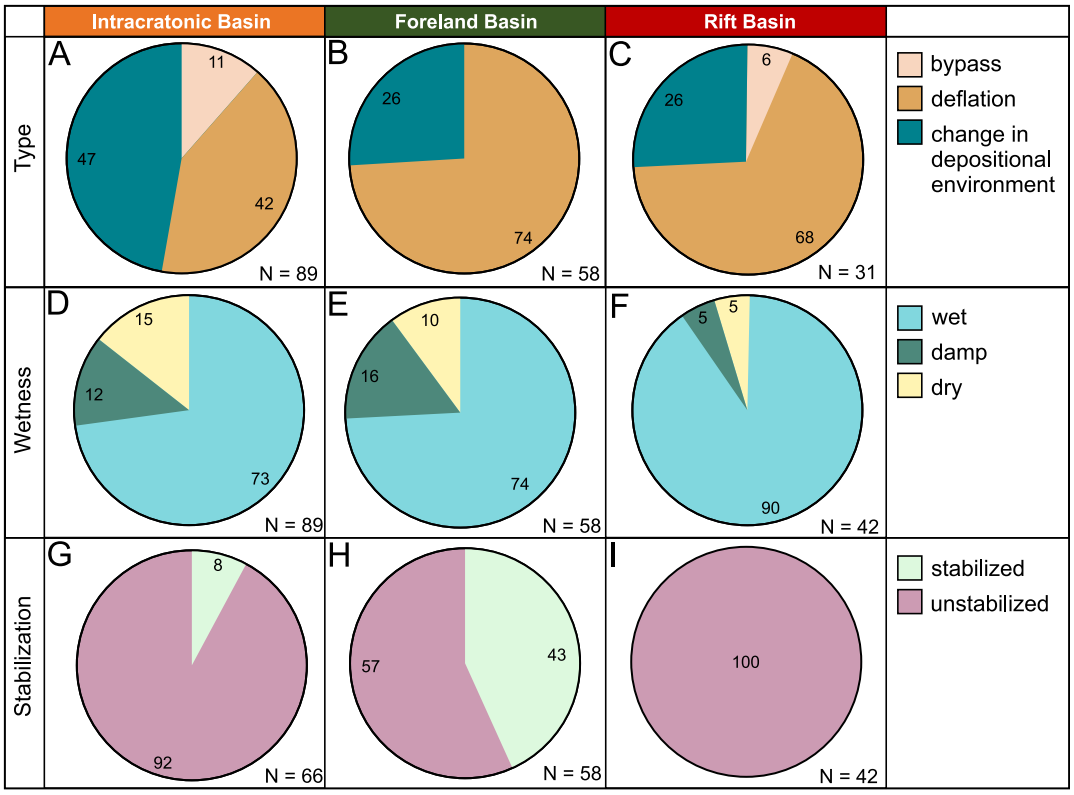

Fig. 8. Qualitative information relating to supersurfaces. A-E) supersurface type (sensu Fryberger, 1993; Kocurek, 1996); F-J) supersurface wetness (ascertained from sedimentary features indicative of substrate conditions); K—O) supersurface stabilization (ascertained from sedimentary features indicating the presence of absence of surface stabilization).

types in modern basin settings may support the assertion that dunes in ancient rift basins tend to be of a smaller average size than dunes found in foreland and intracratonic basins.

Smaller dunes, such as those suggested to be found in rift basins, tend to migrate (i.e. undergo horizontal translation) more rapidly (Mountney and Thompson, 2002; Mountney, 2006; Mountney, 2012; Gunn et al., 2022). Despite the typically rapid rates of subsidence in rift basins, higher dune migration rates may result in lower angles of climb (Mountney, 2012; Jones et al., 2016). Alongside the small size of the formative dunes, such low climb angles may result in the preservation of relatively thin dune sets in the fills of rift basins (Fig. 6B).

Smaller formative dunes that migrate rapidly typically (1) have steep-fronted lee slopes with preserved foresets inclined close to the angle of repose for dry sand, and (2) lack broad, low-angle inclined plinths, resulting in the preservation of a relatively larger fraction of grainflow avalanche strata and relatively less wind-ripple strata (Romain and Mountney, 2014). The dominance in rift basins of small, rapidly migrating aeolian dunes is supported by the facies distributions and internal geometries of aeolian dune sets in rift basins, such that: (1) dune-set elements of rift basins have the highest median foreset dip (inclination) (Table 5); (2) interfingered packages of grainfall and grainflow (dune foreset) form a greater proportion of recorded facies types in dune-set elements of rift basins, relative to those of intracratonic and foreland basins (Fig. 5E); this likely indicates that a greater proportion of grainflow and grainfall strata extend down close to the bases of dune sets, as is typical of small, rapidly migrating dunes (cf. Hunter, 1977; Romain and Mountney, 2014; Nield et al., 2017).

Notwithstanding the above discussion, it is also important to note that the distribution of aeolian stratal types (i.e. packages of grainfall, grainflow and wind-ripple strata) in dune sets can be subject to preservational biases. If only the basalmost parts of dune sets are preserved, for example due to post-depositional reworking, then internal facies distributions preserved within these sets may not be a true reflection of the original dominance of processes active over the full height of a migrating bedform. This is evident, for example, in the lowermost beds of the Page Sandstone (Jones and Blakey, 1997), where lateral changes in dune-set preservation reveal prominent facies changes. In places dune-sets of the Page Sandstone appear to be predominantly composed of wind-ripple strata (i.e. dune toesets); yet, where these beds can be traced laterally, these dune toeset deposits pass into dune foresets composed dominantly of grainflow strata (Jones and Blakey, 1997).

The relatively rapid rates of basin subsidence in rift basins may result in accommodation generation that outpaces sediment supply (e.g., De Almeida et al., 2009). As the sediment supply is outpaced, sand seas (ergs) may become sediment starved, for example due to a relatively high water table, resulting in the formation of relatively small and rapidly migrating dunes (Kocurek and Lancaster, 1999; Mountney, 2012), the deposits of which are then preserved as thin dune sets in the geological record. Moreover, in supply-limited systems where the water table lies close to the accumulation surface, the draw-up of moisture from the shallow subsurface (e.g., Hotta et al., 1984) can maintain a damp or wet surface that traps sand and renders it unavailable for transport and dune construction (Kocurek and Fielder, 1982; Olsen et al., 1989). This process is also common in aeolian systems developed in humid climates (e.g., Mountney and Russell, 2009). These conditions may be satisfied in rift basins where the highest percentage of damp interdunes are found (Fig. 5C).

4.2. *Water table*

Aeolian accumulation is commonly influenced by the presence of water in the system. Both absolute and relative water-level changes can occur: the former may occur in response to changes in climatic conditions, whereas the latter may occur by the subsidence of a sediment accumulation through a water table that is itself static in an absolute sense (Kocurek and Havholm, 1993; Fig. 2). The level of the water table

is controlled by multiple factors on a basin-wide scale (Kocurek, 1981; Hummel and Kocurek, 1984; Kocurek and Havholm, 1993), including bedrock geology, subsidence, sea level, climate, and changes thereof (Kocurek et al., 2001). Given that the temporal position of the water-table may vary in response to complex interactions between the aforementioned variables, relating the position of the water-table to basin setting is challenging. However, some general comments can be made.

In foreland basins, the preservation of thick dune-set and interdune elements may be partly related to shallower (on average) water tables. Relatively high water tables, in combination with high rates of subsidence (Fig. 4B), can result in the rapid sequestration of aeolian deposits beneath the erosional baseline, which is commonly controlled by the level of the water table (Fig. 2). Such sequestration protects aeolian deposits from post-depositional reworking and deflation (Kocurek and Havholm, 1993; Mountney and Russell, 2009; Cosgrove et al., 2021b). Shallow water tables in foreland basins are supported by the proportion of the accumulation represented by wet interdune deposits, which is higher than in any other basin type (Fig. 5C). The inference of overall shallower water tables is also supported by the percentage of sabkha and playa elements, which form a greater fraction of strata of non-aeolian origin in the studied foreland basins than in any other investigated tectonic settings (Fig. 5D). Sabkhas form where the water table or its capillary fringe intersects the accumulation surface; playa lakes form where the water table rises above the level of the accumulation surface for a protracted period (Evans et al., 1964; Purser and Evans, 1973; Herries and Cowan, 1997).

Inhibited aeolian deflation in foreland basins – arising from the rapid sequestration of aeolian sediment beneath the water table – is supported by the limited thickness and proportion of sandsheet elements (Table 5; Figs. 5B & 6C). This is significant because sandsheets may represent the erosional remnants of landforms of originally higher relief, i.e. dunes (Kocurek and Nielson, 1986; Nielson and Kocurek, 1986; Pye and Tsoar, 1990; Mountney and Russell, 2004, 2009).

Contrastingly, the relatively slow subsidence rates documented in intracratonic basins may result in low rates of relative rises in the water table (Fig. 2E). Additionally, the absolute level of the water table may be depressed in intracratonic sags developed in continental interior settings, since the aquifers of such regions tend to experience more limited groundwater recharge by major water bodies or precipitation (e.g., Garven, 1995). Evidence to argue for depressed water-table levels that were markedly below the accumulation surface includes the prevalence of dry interdune elements and dry-type supersurfaces in the fills of intracratonic basins (Fig. 5C & 8D).

Relatively depressed water tables in intracratonic basins, resulting in accumulated deposits lying above the erosional baseline, may contribute to the preservation of relatively thin dune sets and genetic aeolian units in intracratonic basins (Tables 5 & 6; Fig. 6B), since the probability of post-depositional reworking is increased (Kocurek and Havholm, 1993; Mountney and Russell, 2009; Cosgrove et al., 2022a). Greater post-depositional reworking of aeolian dune accumulations is supported by the relatively high proportion of aeolian sandsheet elements in intracratonic basins (Fig. 5B), some of which may represent the erosional remnants of dune landforms of originally higher relief (Kocurek and Nielson, 1986; Nielson and Kocurek, 1986; Pye and Tsoar, 1990; Mountney and Russell, 2004).

4.3. Subsidence histories

The architecture of aeolian successions may partly relate to the subsidence histories of the formative basins in which they are found. The subsidence histories of intracratonic basins are temporally variable and commonly punctuated by episodes when subsidence stalled, else by brief episodes of uplift (e.g., Brunet and Le Pinchon, 1982; Prijac et al., 2000; Fig. 1B). The recorded aeolian architectures of intracratonic basins may reflect such discontinuous histories of subsidence and indicate the sporadic accumulation of aeolian genetic units separated by long episodes of sediment bypass under conditions of low rates of accommodation generation (Table 6; cf. Shaw et al., 1991; Aspler and Chiarenzelli, 1997). Frequent hiatuses in aeolian accumulation are supported by the nature of recorded supersurfaces: a higher proportion of supersurfaces in intracratonic basins have features indicative of bypass, compared to those of other basin settings (Fig. 8A). Bypass supersurfaces represent and record interruptions in aeolian accumulation (e.g., Loope, 1985). Supersurfaces commonly embody significantly more time than the aeolian accumulations themselves (Ager, 1976; Sadler, 1981; Loope, 1985; Havholm and Kocurek, 1994; Mountney, 2006). Frequent hiatuses in aeolian accumulation, associated with bypass supersurfaces, may account for the relatively large amount of time embodied by the aeolian stratigraphy found with intracratonic basins (Fig. 4D), yet the relative thinness of the aeolian stratigraphy developed in these basin types (Fig, 4C).

In intracratonic and foreland basins, the vertical thickness of an aeolian element is likely to be a poor predictor of its lateral extent (Fig. 7A-B). In intracratonic basins, the weak scaling relationships between length and thickness may arise as a consequence of basin subsidence histories, such that episodic uplift and hiatuses in subsidence leave aeolian elements vulnerable to later partial (or complete) erosion and re-working. Such deflation may reduce the original thickness of aeolian elements and may therefore erase positive scaling relationships that may otherwise arise between aeolian element length and thickness. In foreland basins, there is no relationship between aeolian element length and thickness (Fig. 7B), despite relatively rapid rates of basin subsidence (Fig. 4B). This lack of scaling relationship may reflect the shape of foreland basins, which are highly asymmetrical and form an elongate region of potential sediment accommodation (DeCelles and Giles, 1996). The laterally restricted nature of many foreland basins may limit the lateral extent of developing aeolian dune field successions; moreover, the asymmetry of these basin types results in spatially variable subsidence rates that change between the foredeep and the peripheral bulge (DeCelles and Giles, 1996). Furthermore, in foreland basins, the locus of accumulation and erosion can vary through time as subsidence and uplift changes between the foredeep and back-bulge, generating apparently contrasting stratigraphies in different parts of the same basin (Catuneanu et al., 1998, 1999).

In contrast, architectural elements within rift basins show strong vertical and lateral scaling relationships (Fig. 7C). This is likely to arise as a function of rapid sequestration beneath the erosional baseline, associated with high rates of subsidence (Fig. 4B) and relatively shallow water tables (Fig. 5C). In rift basins, the relative thinness of sandsheets (Fig. 6C) indicates that the effects of post-depositional deflation may be more limited (Kocurek and Nielson, 1986; Nielson and Kocurek, 1986), and this may provide explanation for the stronger scaling relationships between aeolian element length and thickness (Fig. 7C).

4.4. Interactions with contiguous non-aeolian systems

Non-aeolian elements that interdigitate with aeolian deposits are most common in rift basins as a total fraction of stratigraphy (Fig. 5A). This indicates the frequent vertical stacking and lateral juxtaposition of aeolian and non-aeolian elements and common changes in depositional environment. Such changes in depositional environment may be driven by climatic shifts at a variety of frequencies (e.g., shifts between glacial and interglacial conditions, or shifts been more arid icehouse and more humid greenhouse conditions; Cosgrove et al., 2021b). However, changes in depositional environment can also be related to basin physiography and subsidence histories.

In rift basins, the high percentage of non-aeolian alluvial and fluvial elements is likely associated with the following: (1) extensional faulting and associated rift-basin subsidence during basin development, which can trigger the generation of alluvial conglomeratic and sandstone bodies that build out from fault-bounded basin margins (e.g., Hadlari et al., 2006; Leleu and Hartley, 2018); and (2) high rates of orographic

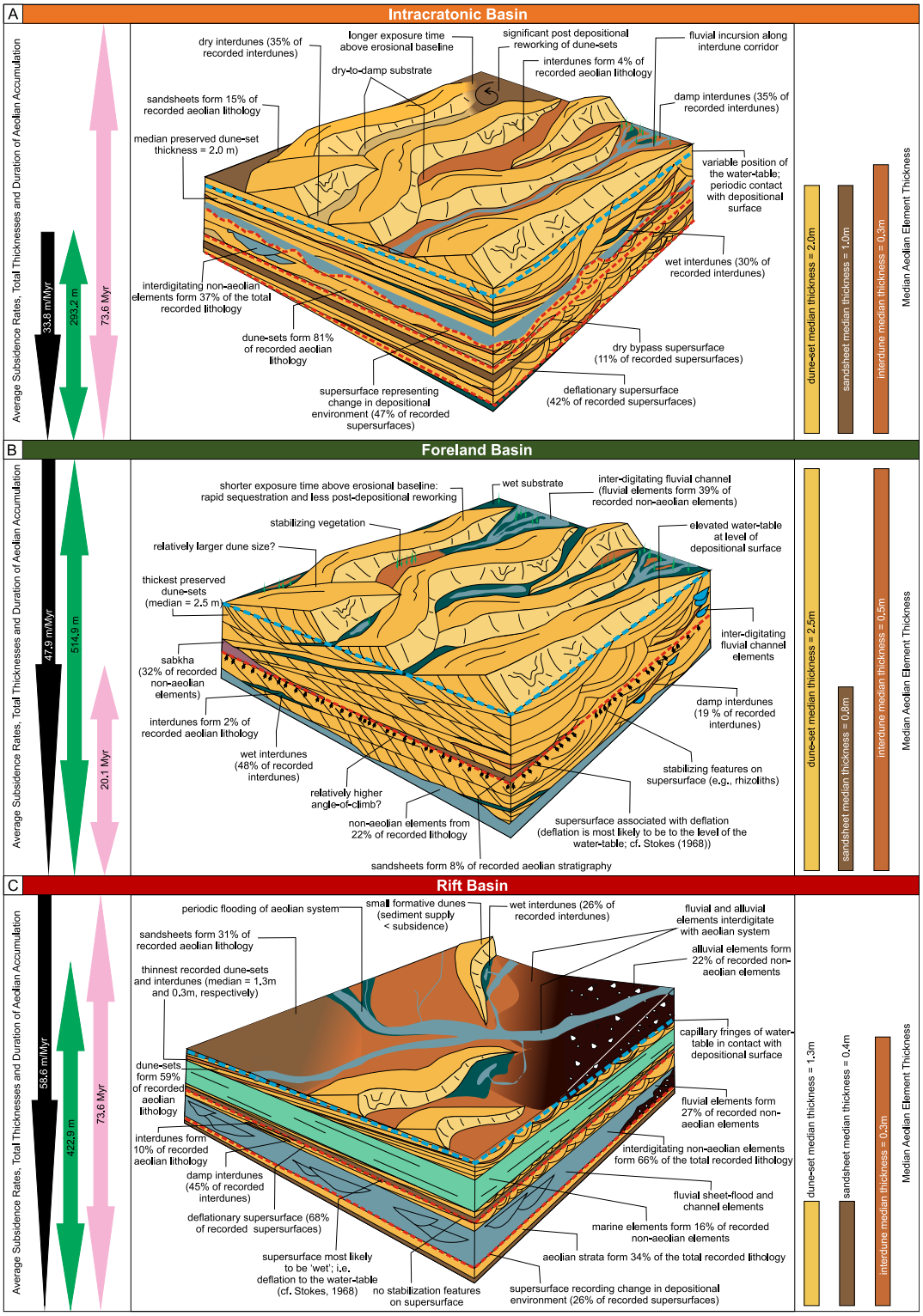

Fig. 9. Facies models based on the quantitative data presented in the text for the five basin types considered here. A) Intracratonic basins; B) foreland basins; and C) rift basins. In all diagrams, the arrows on the left-hand side of the diagram indicate the relative rates of basin subsidence (black arrow), case study thickness (green arrow), and duration of aeolian accumulation (red arrow) across the basin types, as indicated by the different arrow sizes. In all diagrams, the bars on the right hand side of the diagram indicate the relative thickness of dune-sets, sandsheets and interdunes across all basin types, as indicated by the size of the bar. (For interpretation of the references to colour in this figure legend, the reader is referred to the web version of this article.)

precipitation (Barry, 1981; Sing and Kumar, 1997), resulting in enhanced precipitation on the windward side of a topographic barrier (such as the elevated footwall of an underfilled rift basin), and which might feed fluvial systems.

Additionally, in rift basins, aeolian architectures house the highest percentage of sandsheets, relative to all other basin settings (Fig. 5B). The frequent presence of sandsheet elements indicates that conditions outside the range within which dunes can form were prevalent in the

studied rift basins. Kocurek and Nielson (1986) suggest that periodic flooding can favour the construction of aeolian sandsheet over dune fields: frequent inundation by non-aeolian aqueous agents curtails dune construction and instead facilitates the formation of aeolian sandsheets (Fig. 5A, B & D).

In foreland basins, deposition in aeolian systems can also be influenced by orographic precipitation, most notably by feeding fluvial systems (Barry, 1981; Sing and Kumar, 1997). However, in the studied foreland basins, interdigitating non-aeolian elements form the lowest proportion of the total recorded thickness of all basin types (Fig. 5A). In some instances, the interdigitation of non-aeolian elements may be inhibited in foreland basins by shallow water tables, as indicated by the highest percentage of wet interdunes (Fig. 5C). The presence of shallower water tables is typically associated with the development of damp and wet substrates, which can, in some circumstances, promote the formation of biogenic (e.g., vegetation or biogenic films) and chemical (e.g., chemical crust) stabilizing agents under certain palaeoenvironmental conditions (e.g. Byrne and McCann, 1989; Ruz and Allard, 1994; Basilici et al., 2009, 2020). The greater likelihood of encountering stabilizing agents in foreland basins is supported by the sedimentary features of supersurfaces; the highest percentage of supersurfaces associated with stabilizing agents is reported for foreland basins (Fig. 8H). The relatively greater presence of stabilizing agents associated with damp and wet substrates in foreland basins may inhibit the interdigitation of non-aeolian elements by reducing river mobility through channel-bank stabilization; this reduces the potential for river systems to wander across and rework contiguous aeolian deposits (Davies and Gibling, 2010; Al-Masrahy and Mountney, 2015; Santos et al., 2019; Reis et al., 2022).

Notwithstanding the stabilizing effects of vegetation, there are some notable examples of marginal-erg systems that interdigitate repeatedly with non-aeolian elements in the fills of foreland basins. For example, considering outcrops of the Colorado Plateau, some well-known aeolian-dominated systems grade laterally into non-aeolian-dominated systems (e.g., Blakey et al., 1988; Middleton and Blakey, 1983; Mountney and Jagger, 2004). Examples include: (1) parts of the Permian Schnebly Hill Formation, which changes from being composed of ca. 80% aeolian strata at Sedona, Arizona, to being sabkha dominated over a distance of 15 km (Blakey and Middleton, 1983; Blakey, 1990); (2) the Jurassic Page Sandstone, which grades laterally into, and intertongues with, the marine, sabkha and fluvial deposits of the Carmel Formation (Blakey et al., 1996); (3) the Jurassic Navajo Sandstone, which grades laterally into the fluvial- and sabkha-dominated Kayenta Sandstone (Herries, 1993).

5. Conclusions

The accumulation of aeolian-dominated sedimentary successions developed in intracratonic basins, foreland basins, and rift basins are analysed. The summary statistics presented here provide an additional way to predict the architecture of aeolian successions according to the type of basin in which they are found. The data presented here can be used to supplement regional stratigraphic studies, and may be a powerful way to examine such differences.

The main findings of this investigation are summarized as follows:

1) The studied intracratonic basins are characterized by slow generation of accommodation, favouring the accumulation and preservation of relatively thin aeolian genetic units, generated by aeolian dunes that likely climbed at low angles (Fig. 9A). Subsidence histories of most intracratonic basins are characterized by some episodes of no subsidence and even some episodes of minor uplift. Furthermore, intracratonic basins can be sites of repeated marine incursions that dominate these areas over extended periods of time. Such conditions generate punctuated accumulation of aeolian genetic units separated by long episodes of sediment bypass (and potentially of deflation) under conditions of low rates of accommodation generation. In this context, some aeolian accumulations may remain exposed above relatively depressed water tables, making them vulnerable to post-depositional reworking (Fig. 9A).
2) The studied foreland basins record the second highest subsidence rates, and record the thickest dune-set and interdune elements. Relatively high angles of bedform climb are related to sand supply and wind regime; high rates of sediment supply are provided by the erosion of neighbouring orogenic belts, which facilitates the formation of large formative dunes that climb at relatively high angles (Fig. 9B). Elevated water tables, in combination with rapid subsidence rates, allow aeolian accumulations to be placed rapidly beneath the erosional baseline, thereby inhibiting opportunities for post-depositional reworking and deflation.
3) The studied rift basins are characterized by the highest subsidence rates; nonetheless, dune sets and interdunes are thinner, on average, than in the other basin settings. Sediment supply and wind regime are controlling factors; rapid subsidence outpaces sediment supply leading to the formation of small formative dunes (Fig. 9C) that undergo rapid lateral migration and therefore climb at low angles, despite rapid subsidence rates. Rift basins record the highest proportion of sandsheet and non-aeolian elements as a percentage of the total recorded lithology; this is likely a result of prevailing conditions that are not favourable for the construction of larger dunes and dune fields; high water tables and periodic flooding favour the development of sandsheets and the frequent interdigitation of non-aeolian elements (e.g., fluvial, alluvial and marine elements; Fig. 9C).
4) Aeolian deposits can only be preserved in the long-term geological record with basin subsidence (except in cases of exceptional preservation – by volcanic burial, for example). This study highlights the complexity and variability of the aeolian sedimentary fills of various tectonic basin types, each characterized by different subsidence histories and basin physiographies. Sediment supply, readily available corridors of sand transport, wind regime and climate are also paramount. Notwithstanding the potential variability observed between aeolian successions, the results presented here can be applied to guide interpretations and predictions of the architecture of ancient aeolian successions, both in outcrop and in the subsurface, where aeolian strata act as hydrocarbon reservoirs, potential repositories for carbon capture and storage (CCS), hosts of geothermal energy, and as potable water aquifers.

Declaration of Competing Interest

The authors declare that they have no known competing financial interests or personal relationships that could have appeared to influence the work reported in this paper.

Data availability

A supplementary information file is attached showing the raw data used in the investigtaion

Acknowledgements

We thank the sponsors and partners of FRG-ERG-SMRG for financial support for this research: AkerBP, Areva (now Orano), BHP, Cairn India (Vedanta), Chevron, ConocoPhillips, CNOOC, Equinor, Murphy Oil, Occidental, Petrotechnical Data Systems, Aramco, Shell, Tullow Oil, Woodside and YPF. Claiton Scherer and one anonymous reviewer are thanked for their useful comments; we also thank the Editor Christopher Fielding.

Appendix A. Supplementary data

Supplementary data to this article can be found online at https://doi.

org/10.1016/j.earscirev.2022.104293.

References

Abdelsalam, M.G., Liégeois, J.-P., Stern, R.J., 2002. The Saharan Metacraton. J. Afr. Earth Sci. 34, 119–136. https://doi.org/10.1016/S0899-5362(02)00013-1.

Ager, D.V., 1976. The nature of the fossil record. Proc. Geol. Ass. 87, 131–159. https://doi.org/10.1016/S0016-7878(76)80007-7.

Ahlbrandt, T.S., Andrews, S., Gwynne, D.T., 1978. Bioturbation in eolian deposits. J. Sed. Petrol. 48, 839–848. https://doi.org/10.1306/212F7586-2B24-11D7-8648000102C1865D.

Al-Masrahy, M.A., Mountney, N.P., 2015. A classification scheme for fluvial–aeolian system interaction in desert-margin settings. Aeolian Res. 17, 67–88. https://doi.org/10.1016/j.aeolia.2015.01.010.

Allen, J.R.L., 1963. The classification of cross-stratified units. With notes on their formation. Sedimentology 2, 93–114. https://doi.org/10.1111/j.1365-3091.1963.tb01204.x.

Allen, P.A., Allen, J.R.L., 2013. Basin Analysis: Principles and Application to Petroleum Play Assessment. Wiley-Blackwell, Oxford.

Allen, P.A., Armitage, J.J., 2012. Cratonic Basins. In: Busby, C., Azor, A. (Eds.), Tectonics of Sedimentary Basins: Recent Advances. Wiley-Blackwell, Oxford, pp. 602–620. https://doi.org/10.1002/9781444347166.ch30.

Ashley, G.M., Renaut, R.W., 2002. Rift sedimentation. In: Renaut, R.W., Ashley, G.M. (Eds.), Sedimentation in Continental Rifts, 73. SEPM Spec. Pub, pp. 3–7. https://doi.org/10.2110/pec.02.73.

Aspler, L.B., Chiarenzelli, J.R., 1997. Initiation of 2.45–2.1 Ga intracratonic basin sedimentation of the Hurwitz Group, Keewatin Hinterland, Northwest Territories, Canada. Precambrian Res. 81, 265–297. https://doi.org/10.1016/S0301-9268(96)00038-1.

Baas, J.H., McCaffrey, W.D., Knipe, R.J., 2005. The Deep-Water Architecture Knowledge Base: towards an objective comparison of deep-marine sedimentary systems. Petrol. Geosci. 11, 309–320. https://doi.org/10.1144/1354-079304-642.

Bállico, M.B., Scherer, C.M.S., Mountney, N.P., Souza, E.G., Chemale, F., Pisarevsky, S.A., Reis, A.D., 2017. Wind-pattern circulation as a palaeogeographic indicator: Case study of the 1.5-1.6 Ga Mangabeira Formation, Sao Francisco Craton, Northeast Brazil. Precambrian Res. 298, 1–15. https://doi.org/10.1016/j.precamres.2017.05.005.

Barry, R.G., 1981. In: Mountain Weather and Climate. Metheun, London, p. 313.

Bart, H.A., 1977. Sedimentology of cross-stratified sandstones in Arikaree Group, Miocene, Southeastern Wyoming. Sed. Geol. 19, 165–184. https://doi.org/10.1016/0037-0738(77)90029-X.

Basilici, G., Fuhr-Dal, B.P.F., Ladeira, F.S.B., 2009. Climate-induced sediment-palaeosol cycles in a late cretaceous dry aeolian sand sheet; Marilia Formation (north-West Bauru Basin, Brazil). Sedimentology 56, 1876–1904. https://doi.org/10.1111/j.1365-3091.2009.01061.x.

Basilici, G., Soares, M.V.T., Mountney, N.P., Colombera, L., 2020. Microbial influence on the accumulation of Precambrian aeolian deposits (Neoproterozoic, Venkatpur Sandstone Formation, Southern India). Precambrian Res. 347, 105854 https://doi.org/10.1016/j.precamres.2020.105854.

Benan, C.A.A., Kocurek, G., 2000. Catastrophic flooding of an aeolian dune field: Jurassic Entrada and Todilto Formations, ghost Ranch, New Mexico, USA. Sedimentology 47, 1069–1080. https://doi.org/10.1046/j.1365-3091.2000.00341.x.

Benison, K.C., Knapp, J.P., Dannenhoffer, J.M., 2011. The Pennsylvanian Pewamo Formation and associated Haybridge strata; toward the resolution of the Jurassic Ionia red bed problem in the Michigan Basin, U.S.A. J. Sed. Res. 81, 459–478. https://doi.org/10.2110/jsr.2011.039.

Biswas, A., 2005. Coarse aeolianites: sand sheets and zibar-interzibar facies from the Mesoproterozoic Cuddapah Basin, India. Sed. Geol. 174, 149–160. https://doi.org/10.1016/j.sedgeo.2004.11.005.

Blakey, R.C., 1988. Basin tectonics and erg response. Sed. Geol. 56, 127–151. https://doi.org/10.1016/0037-0738(88)90051-6.

Blakey, R.C., 1990. Stratigraphy and geologic history of Pennsylvanian and Permian rocks, Mogollon Rim region, central Arizona and vicinity. GSA Bull 102, 1189–1217. https://doi.org/10.1130/0016-7606(1990)102<1189:SAGHOP>2.3.CO;2.

Blakey, R.C., Middleton, L.T., 1983. Permian shoreline eolian complex in central Arizona: dune changes in response to cyclic sea-level changes. In: Brookfield, M.E., Ahlbrandt, T.S. (Eds.), Eolian Sediments and Process. Dev. Sedimentol, 38. Elsevier, Amsterdam, pp. 551–581. https://doi.org/10.1016/S0070-4571(08)70813-6.

Blakey, R.C., Havholm, K.G., Jones, L.S., 1996. Stratigraphic analysis of eolian interactions with marine and fluvial deposits, Middle Jurassic Page Sandstone and Carmel Formation, Colorado Plateau, USA. J. Sed. Res. 66, 324–342. https://doi.org/10.1306/D426833D-2B26-11D7-8648000102C1865D.

Blakey, R.C., Peterson, F., Kocurek, G., 1988. Synthesis of late Paleozoic and Mesozoic eolian deposits of the Western Interior of the United States. Sed. Geol. 56, 3–125. https://doi.org/10.1016/0037-0738(88)90050-4.

Breed, C.S., Grow, T., 1979. Morphology and distribution of dunes in sand seas observed by remote sensing. In: McKee, E.D. (Ed.), A Study of Global Sand Seas. United States Government Printing Office, Washington, DC, pp. 253–304.

Brookfield, M.E., 1977. The origin of bounding surfaces in ancient aeolian sandstones. Sedimentology 24, 303–332. https://doi.org/10.1111/j.1365-3091.1977.tb00126.x.

Brunet, M.-F., Le Pinchon, X., 1982. Subsidence of the Paris Basin. J. Geophys. Res. Atmos. 87, 8547–8560. https://doi.org/10.1029/JB087iB10p08547.

Burgess, P.M., 2019. Phanerozoic Evolution of the Sedimentary Cover of the North American Craton. In: Miall, A.D. (Ed.), The Sedimentary Basins of the United States and Canada, Second Edition. Elsevier, pp. 39–75. https://doi.org/10.1016/B978-0-444-63895-3.00002-4.

Byrne, M.-L., McCann, S.B., 1989. Stratification models for vegetated coastal dunes in Atlantic Canada. Sed. Geol. 66, 165–179. https://doi.org/10.1016/0037-0738(90)90058-2.

Catuneanu, O., Hancox, P.G., Rubidge, B.S., 1998. Reciprocal flexural behaviour and contrasting stratigraphies: a new basin development model for the Karoo retroarc foreland system, South Africa. Basin Res. 10, 417–439. https://doi.org/10.1046/j.1365-2117.1998.00078.x.

Catuneanu, O., Sweet, A.R., Miall, A.D., 1999. Concepts and Styles of reciprocal stratigraphies: Western Canada, foreland system. Terra Nova 11, 1–8. https://doi.org/10.1046/j.1365-3121.1999.00222.x.

Chakraborty, T., 1991. Sedimentology of a Proterozoic erg: the Venkatpur Sandstone, Pranhita-Godavari Valley, South-India. Sedimentology 38, 301–322. https://doi.org/10.1111/j.1365-3091.1991.tb01262.x.

Chakraborty, T., Chakraborty, C., 2001. Eolian-aqueous interactions in the development of a Proterozoic sand sheet: Shikaoda Formation, Hosangabad, India. J. Sed. Res. 71, 107–117. https://doi.org/10.1306/031700710107.

Chakraborty, T., Chaudhuri, A.K., 1993. Fluvial-aeolian interactions in a Proterozoic alluvial plain: example from the Mancheral Quartzite, Sullavai Group, Pranhita-Godavari Valley, India. In: Pye, K. (Ed.), The Dynamics and Environmental Context of Aeolian Sedimentary Systems, 72. Geol. Soc. Spec. Pub, pp. 127–141. https://doi.org/10.1144/GSL.SP.1993.072.01.12.

Chakraborty, T., Sensarma, S., 2008. Shallow marine and coastal eolian quartz arenites in the Neoarchean-Palaeoproterozoic Karutola Formation, Dongargarh volcano-sedimentary succession, Central India. Precambrian Res. 162, 284–301. https://doi.org/10.1016/j.precamres.2007.07.024.

Chan, M.A., Kocurek, G., 1988. Complexities in eolian and marine interactions: processes and eustatic controls on erg development. Sed. Geol. 56, 283–300. https://doi.org/10.1016/0037-0738(88)90057-7.

Chrintz, T., Clemmensen, L.B., 1993. Draa reconstruction, the Permian Yellow Sands, northeast England. In: Pye, K., Lancaster, N. (Eds.), Aeolian Sediments. Ancient and Modern, 16. Int. Assoc. Sedimentol. Spec. Publ, pp. 151–161.

Clemmensen, L.B., 1987. Complex star dunes and associated aeolian bedforms, Hopeman Sandstone (Permo-Triassic), Moray Firth Basin, Scotland. In: Frostick, L.E., Reid, I. (Eds.), Desert Sediments: Ancient and Modern, 35. Geol. Soc. London Spec. Pub, pp. 213–231. https://doi.org/10.1144/GSL.SP.1987.035.01.15.

Clemmensen, L.B., 1988. Aeolian morphology preserved by lava cover, the Precambrian Mussartût Member, Eriksfjord Formation, South Greenland. Bull. Geol. Soc. Denmark 37, 105–116.

Clemmensen, L.B., Abrahamsen, K., 1983. Aeolian stratification and facies association in desert sediments, Arran basin (Permian), Scotland. Sedimentology 30, 311–339. https://doi.org/10.1111/j.1365-3091.1983.tb00676.x.

Clemmensen, L.B., Øxnevad, I.E.I., de Boer, P.L., 1994. Climatic controls on ancient desert sedimentation: Some late Palaeozoic examples from NW Europe and the western interior of the USA. In: de Boer, P.L., Smith, D.G. (Eds.), Orbital Forcing and Cyclic Sequences, 19. IAS Spec. Pub, pp. 439–457. https://doi.org/10.1002/9781444304039.ch27.

Cojan, I., Thiry, M., 1992. Seismically induced deformation structures in Oligocene shallow-marine and aeolian coastal sands (Paris Basin). Tectonophysics 206, 78–89. https://doi.org/10.1016/0040-1951(92)90369-H.

Colombera, L., Mountney, N.P., McCaffrey, W.D., 2012. A relational database for the digitization of fluvial architecture concepts and example applications. Pet. Geo. 18, 129–140. https://doi.org/10.1144/1354-079311-021.

Colombera, L., Mountney, N.P., Hodgson, D.M., McCaffrey, W.D., 2016. The Shallow-Marine Architecture Knowledge Store: a database for the characterization of shallow-marine and paralic depositional systems. Mar. Pet. Geol. 75, 83–99. https://doi.org/10.1016/j.marpetgeo.2016.03.027.

Cosgrove, G.I.E., Colombera, L., Mountney, N.P., 2021a. A database of Eolian Sedimentary Architecture for the characterization of modern and ancient sedimentary systems. Mar. Pet. Geol. 127, 104983 https://doi.org/10.1016/j.marpetgeo.2021.104983.

Cosgrove, G.I.E., Colombera, L., Mountney, N.P., 2021b. Quantitative analysis of the sedimentary architecture of eolian successions developed under icehouse and greenhouse climatic conditions. GSA Bull. https://doi.org/10.1130/B35918.1.

Cosgrove, G.I.E., Colombera, L., Mountney, N.P., 2022a. The role of subsidence and accommodation generation in controlling the nature of the aeolian stratigraphic record. J. Geol. Soc. 179 https://doi.org/10.1144/jgs2021-042 jgs2021–042.

Cosgrove, G.I.E., Colombera, L., Mountney, N.P., 2022b. Eolian stratigraphic record of environmental change through geological time. Geology 50, 289–294. https://doi.org/10.1130/G49474.1.

Cowan, G., 1993. Identification and significance of aeolian deposits within the dominantly fluvial Sherwood Sandstone group of the East Irish Sea Basin UK. In: North, C.P., Prosser, D.J. (Eds.), Characterization of Fluvial and Aeolian Reservoirs, 73. Geol. Soc. London Spec. Pub, pp. 231–245. https://doi.org/10.1144/GSL.SP.1993.073.01.14.

Crabaugh, M., Kocurek, G., 1993. Entrada Sandstone: An example of a wet aeolian system. In: Pye, K. (Ed.), The Dynamics and Environmental Context of Aeolian Sedimentary Systems, 72. Geol. Soc. London Spec. Pub, pp. 103–126. https://doi.org/10.1144/GSL.SP.1993.072.01.11.

Dal'Bó, P.F.F., Basilici, G., Angélica, R.S., 2010. Factors of paleosol formation in a Late Cretaceous eolian sand sheet paleoenvironment, Marília Formation, Southeastern Brazil. Palaeogeog. Palaeoclim. Palaeoecol. 292, 349–365. https://doi.org/10.1016/j.palaeo.2010.04.021.

Dasgupta, P.K., Biswas, A., Mukherjee, R., 2005. Cyclicity in Palaeoproterozoic to Neoproterozoic Cuddapah Supergroup and its significance in basinal evolution. In:

Mabesoone, J.M., Neumann, V.H. (Eds.), Cyclic Development of Sedimentary Basins. Dev. Sediment, 57, pp. 313–354. https://doi.org/10.1016/S0070-4571(05)80013-5.
Davies, N.S., Gibling, M.R., 2010. Cambrian to Devonian evolution of alluvial systems: the sedimentological impact of the earliest land plants. Ear. Sci. Rev. 98, 171–200. https://doi.org/10.1016/j.earscirev.2009.11.002.
Davis, J.C., 1986. Statistics and Data Analysis in Geology. John Wiley & Sons Inc., New York.
De Almeida, R.P., Janikian, L., Fragoso-Cesar, A.R.S., Marconato, A., 2009. Evolution of a rift basin dominated by subaerial deposits: the Guaritas Rift, early Cambrian, Southern Brazil. Sed. Geol. 217, 30–51.
DeCelles, P.G., Giles, K.A., 1996. Foreland basin systems. Basin Res. 8, 105–123. https://doi.org/10.1046/j.1365-2117.1996.01491.x.
Deynoux, M., Kocurek, G., Proust, J.N., 1989. Late Proterozoic periglacial aeolian deposits on the West African Platform, Taoudeni Basin, western Mali. Sedimentology 36, 531–550. https://doi.org/10.1111/j.1365-3091.1989.tb02084.x.
Dias, K.D.N., Scherer, C.M.S., 2008. Cross-bedding set thickness and stratigraphic architecture of aeolian systems: an example from the Upper Permian Piramboia Formation (Parana Basin), southern Brazil. J. South Am. Ear. Sci. 25, 405–415. https://doi.org/10.1016/j.jsames.2007.07.008.
Dott, R.H., Byers, C.W., Fielder, G.W., Stenzel, S.R., Winfree, K.E., 1986. Aeolian to marine transition in Cambro-Ordovician cratonic sheet sandstones of the northern Mississippi valley, U.S.A. Sedimentology 33, 345–367. https://doi.org/10.1111/j.1365-3091.1986.tb00541.x.
Einsele, G., 2000. Sedimentary Basins. Evolution, Facies, and Sediment Budget. Springer, Berlin.
El-Baz, F., Breed, C.S., Grolier, M.J., McCauley, J.F., 1979. Eolian features in the western desert of Egypt and some applications to Mars. J. Geophys. Res. 84, 8205–8221. https://doi.org/10.1029/JB084iB14p08205.
Ellis, D., 1993. The Rough Gas Field: distribution of Permian aeolian and non-aeolian reservoir facies and their impact on field development. Geol. Soc. London Spec. Pub. 73, 265–277. https://doi.org/10.1144/GSL.SP.1993.073.01.16.
Evans, G., Kendall, C.G.S.C., Skipwith, P., 1964. Origin of coastal flats, the sabkha of the Trucial Coast, Persian Gulf. Nature 202, 759–761. https://doi.org/10.1038/202759a0.
Ferronatto, J.P.F., Scherer, C.M.S., de Souza, E.G., dos Reis, A.D., de Mello, R.G., 2019. Genetic units and facies architecture of a Lower Cretaceous fluvial-aeolian succession, São Sebastião Formation, Jatobá Basin, Brazil. J. Sou. Am. Ear. Sci. 89, 158–172. https://doi.org/10.1016/j.jsames.2018.11.009.
Fryberger, S.G., 1993. A review of aeolian bounding surfaces, with examples from the Permian Minnelusa Formation, USA. In: North, C.P., Prosser, D.J. (Eds.), Characterization of Fluvial and Aeolian Reservoirs, 73. Geol. Soc. London Spec. Publ, pp. 167–197. https://doi.org/10.1144/GSL.SP.1993.073.01.11.
Fryberger, S.G., Schenk, C.J., Krystinik, L.F., 1988. Stokes surfaces and the effects of near-surface groundwater-table on Aeolian deposition. Sedimentology 35, 21–41. https://doi.org/10.1111/j.1365-3091.1988.tb00903.x.
García-Hidalgo, J.F., Temiño, J., Segura, M., 2002. Holocene eolian sediments on the southern border of the Duero Basin (Spain): origin and development of an eolian system in a temperate zone. J. Sed. Res. 72, 30–39. https://doi.org/10.1306/040501720030.
Garven, G., 1995. Continental-scale groundwater flow and geologic processes. Annu. Rev. Earth Planet. Sci. 23, 89–118. https://doi.org/10.1146/annurev.ea.23.050195.000513.
Gay Jr., S.P., 1999. Observations regarding the movement of barchan sand dunes in the Nazca to Tanaca area of southern Peru. Geomorphology 27, 279–293. https://doi.org/10.1016/S0169-555X(98)00084-1.
Geehan, G., Underwood, J., 1993. The use of length distributions in geological modelling. IAS Spec. Pub. 15, 205–212. https://doi.org/10.1002/9781444303957.ch13.
George, G.T., Berry, J.K., 1997. Permian (Upper Rotliegend) synsedimentary tectonics, basin development and palaeogeography of the southern North Sea. In: Ziegler, P., Turner, P., Daines, S.R. (Eds.), Petroleum Geology of the Southern North Sea, 123. Geol. Soc. London Spec. Pub, pp. 31–61. https://doi.org/10.1144/GSL.SP.1997.123.01.04.
Gibling, M.R., Davies, N.S., 2012. Palaeozoic landscapes shaped by plant evolution. Nature Geosci. 5, 99–105. https://doi.org/10.1038/ngeo1376.
Glennie, K.W., Buller, A.T., 1983. The Permian Weissliegend of North West Europe. The partial deformation of aeolian dune sands caused by the Zechstein transgression. Sed. Geol. 35, 43–81. https://doi.org/10.1016/0037-0738(83)90069-6.
Gregory, J.W., 1894. Contributions to the physical geography of British East Africa. Geogr. J. 4, 289–315. https://doi.org/10.2307/1773534.
Gross, E.C., Carr, M., Jobe, Z.R., 2022. Three-Dimensional Bounding Surface Architecture and Lateral Facies Heterogeneity of a Wet Aeolian System: Entrada Sandstone. Sedimentology, Utah. https://doi.org/10.1111/sed.13035.
Gunn, A., Casasanta, G., Di Liberto, L., Falcini, F., Lancaster, N., Jerolmack, D.J., 2022. What sets aeolian dune height? Nat. Commun. 13, 2401. https://doi.org/10.1038/s41467-022-30031-1.
Hadlari, T., Rainbird, R.H., Donaldson, J.A., 2006. Alluvial, eolian and lacustrine sedimentology of a Paleoproterozoic half-graben, Baker Lake Basin, Nunavut, Canada. Sed. Geol. 190, 47–70. https://doi.org/10.1016/j.sedgeo.2006.05.005.
Hassan, M.S., Venetikidis, A., Bryant, G., Miall, A.D., 2018. The Sedimentology of an ERG margin: the Kayenta-Navajo transition (Lower Jurassic), Kanab, Utah, U.S.A. J. Sed. Res. 88, 613–640. https://doi.org/10.2110/jsr.2018.31.
Havholm, K.G., Kocurek, G., 1994. Factors controlling aeolian sequence stratigraphy: Clues from super bounding surface features in the Middle Jurassic Page Sandstone. Sedimentology 41, 913–934. https://doi.org/10.1111/j.1365-3091.1994.tb01432.x.
Haxby, W.F., Turcotte, D.L., Bird, J.M., 1976. Thermal and mechanical evolution of the Michigan Basin. Tectonophysics 36, 57–75. https://doi.org/10.1016/0040-1951(76)90006-8.
Herries, R.D., 1993. Contrasting styles of fluvio-aeolian interaction at a downwind erg margin: Jurassic Kayenta-Navajo transition, northern Arizona, USA. In: North, C.P., Prosser, D.J. (Eds.), Characterization of Fluvial and Aeolian Reservoirs, 73. Geol. Soc. London Spec. Publ, pp. 199–218. https://doi.org/10.1144/GSL.SP.1993.073.01.12.
Herries, R.D., Cowan, G., 1997. Challenging the 'sheetflood' myth: The role of water-table-controlled sabkha deposits in redefining the depositional model for the Ormskirk Sandstone Formation (Lower Triassic), East Irish Sea Basin. In: Meadows, N.S., Trueblood, S.P., Hardman, M., Cowan, G. (Eds.), 124. Geol. Soc. London Spec. Publ, pp. 253–276. https://doi.org/10.1144/GSL.SP.1997.124.01.16.
Hotta, S., Kubota, S., Katori, S., Horikawa, K., 1984. Sand transport by wind on wet sand surface. Coast. Eng. 2, 1265–1281.
Howell, J.A., Mountney, N.P., 1997. Climatic cyclicity and accommodation space in arid and semi-arid depositional systems: an example from the Rotliegende Group of the southern North Sea. In: North, C.P., Prosser, J.D. (Eds.), Petroleum Geology of the Southern North Sea: Future Potential, 123. Geol. Soc. London Spec. Publ, pp. 199–218. https://doi.org/10.1144/GSL.SP.1997.123.01.05.
Hummel, G., Kocurek, G., 1984. Interdune areas of the Back-Island dune field, North Padre-Island, Texas. Sed. Geol. 39, 1–26. https://doi.org/10.1016/0037-0738(84)90022-8.
Hunter, R.E., 1977. Basic types of stratification in small eolian dunes. Sedimentology 24, 361–387. https://doi.org/10.1111/j.1365-3091.1977.tb00128.x.
Irmen, A.P., Vondra, C.F., 2000. Aeolian sediments in lower to middle (?) Triassic rocks of Central Wyoming. Sed. Geol. 132, 69–88. https://doi.org/10.1016/S0037-0738(99)00129-3.
Nunn, J.A., Sleep, N.H., 1984. Thermal contraction and flexure of intracratonal basins: a three-dimensional study of the Michigan basin. Geophys. J. Int. 76, 587–635. https://doi.org/10.1111/j.1365-246X.1984.tb01912.x.
Jerram, D.A., Mountney, N.P., Howell, J.A., Long, D., Stollhofen, H., 2000. Death of a sand sea: an active aeolian erg systematically buried by the Etendeka flood basalts of NW Namibia. J. Geol. Soc. Lond. 157, 513–516. https://doi.org/10.1144/jgs.157.3.513.
Johnson, P.R., Woldehaimanot, B., 2003. Development of the Arabian–Nubian Shield: perspectives on accretion and deformation in the northern East African Orogen and the assembly of Gondwana. In: Yoshida, M., Windley, B.F., Dasgupta, S. (Eds.), Proterozoic East Gondwana: Supercontinent Assembly and Breakup, 206. Geol. Soc. Lon. Spec. Pub, pp. 289–325.
Jones, L.S., Blakey, R.C., 1997. Eolian-fluvial interaction in the Page Sandstone (Middle Jurassic) in south-Central Utah, USA: a case study of erg-margin processes. Sed. Geol. 109, 181–198. https://doi.org/10.1016/S0037-0738(96)00044-9.
Jones, F.H., Scherer, C.M.S., Kuchle, J., 2016. Facies architecture and stratigraphic evolution of aeolain dune and interdune deposits, Permian Caldeirao Member (Santa Brigida Formation), Brazil. Sediment. Geol. 337, 133–150. https://doi.org/10.1016/j.sedgeo.2016.03.018.
Jordan, O.D., Mountney, N.P., 2010. Styles of interaction between aeolian, fluvial and shallow marine environments in the Pennsylvanian to Permian lower Cutler beds, south-East Utah, USA. Sedimentology 57, 1357–1385. https://doi.org/10.1111/j.1365-3091.2010.01148.x.
Karpeta, W.P., 1990. The morphology of Permian palaeodunes - a reinterpretation of the Bridgnorth Sandstone around Bridgnorth, England, in the light of modern dune studies. Sed. Geol. 69, 59–75.
Klein, G.V., Hsui, A.T., 1987. Origin of cratonic basins. Geology 15, 1094–1098. https://doi.org/10.1130/0091-7613(1987)15<1094:OOCB>2.0.CO;2.
Kocurek, G., 1981. Significance of interdune deposits and bounding surfaces in eolian dune sands. Sedimentology 28, 753–780. https://doi.org/10.1111/j.1365-3091.1981.tb01941.x.
Kocurek, G., 1988. First-order and super bounding surfaces in eolian sequences – Bounding surfaces revisited. Sed. Geol. 56, 193–206. https://doi.org/10.1016/0037-0738(88)90054-1.
Kocurek, G., 1996. Desert aeolian systems. In: Reading, H.G. (Ed.), Sedimentary Environments: Processes, Facies and Stratigraphy, 3rd edition. Blackwell, Oxford, pp. 125–153.
Kocurek, G., 1999. The aeolian rock record (Yes, Virginia, it exists but it really is rather special to create one). In: Goudie, A.S., Livingstone, I., Stokes, S. (Eds.), Aeolian Environments Sediments and Landforms. John Wiley and Sons Ltd, Chichester, pp. 239–259.
Kocurek, G., Day, M., 2018. What is preserved in the aeolian rock record? A Jurassic Entrada Sandstone case study at the Utah-Arizona border. Sedimentology 65, 1301–1321. https://doi.org/10.1111/sed.12422.
Kocurek, G., Fielder, G., 1982. Adhesion structures. J. Sediment. Petrol. 52, 1229–1241. https://doi.org/10.1306/212F8102-2B24-11D7-8648000102C1865D.
Kocurek, G., Havholm, K.G., 1993. Eolian sequence stratigraphy-a conceptual framework. In: Weimer, P., Posamentier, H. (Eds.), Siliciclastic Sequence Stratigraphy, 58. AAPG Mem, pp. 393–409. https://doi.org/10.1306/M58581C16.
Kocurek, G., Lancaster, N., 1999. Aeolian system sediment state: theory and Mojave Desert Kelso dune field example. Sedimentology 46, 505–515. https://doi.org/10.1046/j.1365-3091.1999.00227.x.
Kocurek, G., Nielson, J., 1986. Conditions favourable for the formation of warm-climate aeolian sand sheets. Sedimentology 33, 795–816. https://doi.org/10.1111/j.1365-3091.1986.tb00983.x.
Kocurek, G., Knight, J., Havholm, K., 1991. Outcrop and semi-regional three-dimensional architecture and reconstruction of a portion of the eolian Page Sandstone (Jurassic). In: Miall, A.D., Tyler, N. (Eds.), The Three-Dimensional Facies Architecture of

Terrigenous Clastic Sediments and Its Implications for Hydrocarbon Discovery and Recovery. https://doi.org/10.2110/csp.91.03.0025.
Kocurek, G., Robinson, N.I., Sharp, J.M.J., 2001. The response of the water table in coastal aeolian systems to changes in sea level. Sed. Geol. 139, 1–13. https://doi.org/10.1016/S0037-0738(00)00137-8.
Krapovickas, V., Mángano, M.G., Buatois, L.A., Marsicano, C.A., 2016. Integrated Ichnofacies models for deserts: Recurrent patterns and megatrends. Earth Sci. Rev. 157, 61–85. https://doi.org/10.1016/j.earscirev.2016.03.006.
Lancaster, N., 1985. Winds and sand movements in the Namib sand sea. Ear. Surf. Proc. Landf. 10, 607–619. https://doi.org/10.1002/esp.3290100608.
Lancaster, N., 1992. Relations between dune generations in the Gran Desierto, Mexico. Sedimentology 39, 631–644. https://doi.org/10.1111/j.1365-3091.1992.tb02141.x.
Lancaster, N., Teller, J.T., 1988. Interdune deposits of Namib Sand Sea. Sed. Geol. 55, 91–107. https://doi.org/10.1016/0037-0738(88)90091-7.
Langford, R.P., Chan, M.A., 1988. Flood surfaces and deflation surfaces within the Cutler Formation and Cedar Mesa Sandstone (Permian), southeastern Utah. Geol. Soc. Am. Bull. 100, 1541–1549. https://doi.org/10.1130/0016-7606(1988)100<1541:FSADSW>2.3.CO;2.
Lee, E.Y., Novotny, J., Wagreich, M., 2019. Subsidence Analysis and Visualization. Springer Briefs in Petroleum Geoscience and Engineering. Springer International Publishing. https://doi.org/10.1007/978-3-319-76424-5, 1–56 pp.
Leeder, M., 2011. Sedimentology and Sedimentary Basins: From Turbulence to Tectonics. Wiley, Chichester.
Leleu, S., Hartley, A.J., 2010. Controls on the stratigraphic development of the Triassic Fundy Basin, Nova Scotia; implications for the tectonostratigraphic evolution of Triassic Atlantic rift basins. J. Geol. Soc. 167, 437–454. https://doi.org/10.1144/0016-76492009-092.
Leleu, S., Hartley, A.J., 2018. Constraints on synrift intrabasinal horst development from alluvial fan and aeolian deposits (Triassic, Fundy Basin, Nova Scotia). In: Ventra, D., Clarke, L.E. (Eds.), Geology and Geomorphology of Alluvial and Fluvial Fans: Terrestrial and Planetary Perspectives, 440. Geol. Soc. London Spec. Pub, pp. 79–101. https://doi.org/10.1144/SP440.8.
Liesa, C.L., Rodríguez-López, J.P., Ezquerro, L., Alfaro, P., Rodriguez-Pascua, M.A., Lafuente, P., Arlegui, L., Simon, J.L., 2016. Facies control on seismites in an alluvial-aeolian system: the Pliocene dunefield of the Teruel half-graben basin (eastern Spain). Sed. Geol. 344, 237–252. https://doi.org/10.1016/j.sedgeo.2016.05.009.
Loope, D.B., 1985. Episodic deposition and preservation of eolian sands – a late Paleozoic example from southeastern Utah. Geology 13, 73–76. https://doi.org/10.1130/0091-7613(1985)13<73:EDAPOE>2.0.CO;2.
Loope, D.B., 1988. Rhizoliths and ancient aeolianites. Sed. Geol. 56, 301–314. https://doi.org/10.1016/0037-0738(88)90058-9.
Loope, D.B., Rowe, C.M., 2003. Long-lived pluvial episodes during deposition of the Navajo Sandstone. J. Geol. 111, 223–232. https://doi.org/10.1086/345843.
Loope, D.B., Swinehart, J.B., Mason, J.P., 1995. Dune-dammed paleovalleys of the Nebraska Sand Hills- intrinsic versus climatic controls on the accumulation of lake and marsh sediments. Geol. Soc. Am. Bull. 107, 396–406. https://doi.org/10.1130/0016-7606(1995)107<0396:DDPOTN>2.3.CO;2.
Mack, G.H., 1978. Tectonic control of sedimentation. In: Middleton, G.V., Church, M.J., Coniglio, M., Hardie, L.A., Longstaffe, F.J. (Eds.), Encyclopedia of Sediments and Sedimentary Rocks. Encyclopedia of Earth Sciences Series. Springer, Dordrecht. https://doi.org/10.1007/978-1-4020-3609-5_235.
MacNaughton, R.B., Cole, J.M., Dalrymple, R.W., Braddy, S.J., Briggs, D.E.G., Lukie, T. D., 2002. First steps on land: Arthropod trackways in Cambrian-Ordovician eolian sandstone, southeastern Ontario, Canada. Geology 30, 391–394. https://doi.org/10.1130/0091-7613(2002)030<0391:FSOLAT>2.0.CO;2.
Mascle, A., Puigdefabregas, C., 1998. Tectonics and sedimentation in foreland basins: results from the Integrated Basin Studies project. In: Mascle, A., Puigdefabregas, C., Luterbacher, H.P., Fernandez, M. (Eds.), Cenozoic Foreland Basins of Western Europe, 134. Geol. Soc. Spec. Pub, pp. 1–28. https://doi.org/10.1144/GSL.SP.1998.134.01.02.
McKee, E.D., 1979. In: A Study of Global Sand Seas, 1052. United States Department of the Interior, US Geological Survey Professional Paper, p. 429.
Meadows, N.S., Beach, A., 1993. Structural and climatic controls on facies distribution in a mixed fluvial and aeolian reservoir: the Triassic Sherwood Sandstone in the Irish Sea. In: North, C.P., Prosser, D.J. (Eds.), Characterization of Fluvial and Aeolian Reservoirs, 73. Geol. Soc. London Spec. Pub, pp. 247–264. https://doi.org/10.1144/GSL.SP.1993.073.01.15.
Melton, M.A., 1965. The geomorphic and paleoclimatic significance of alluvial deposits in southern Arizona. J. Geol. 73, 1–38. http://www.jstor.org/stable/30066379.
Melvin, J., Sprague, R.A., Heine, C.J., 2010. From bergs to ergs: The late Paleozoic Gondwanan glaciation and its aftermath in Saudi Arabia. In: López-Gamundí, O.R., Buatois, L.A. (Eds.), Late Paleozoic Glacial Events and Postglacial Transgressions in Gondwana, 468. Geol. Soc. America Spec. Paper, pp. 37–80. https://doi.org/10.1130/2010.2468(02).
Miall, A.D., 1985. Architectural-Element Analysis: a New Method of Facies Analysis Applied to Fluvial Deposits. Earth Sci. Rev. 22, 261–308. https://doi.org/10.1016/0012-8252(85)90001-7.
Miall, A.D., 2000. Principles of Sedimentary Basin Analysis. Springer, Berlin.
Middleton, M.F., 1989. A model for the formation of intracratonic sag basins. Geophys. J. Int. 99, 665–676. https://doi.org/10.1111/j.1365-246X.1989.tb02049.x.
Middleton, L.T., Blakey, R.C., 1983. Process and controls on the intertonguing of the Kayenta and Navajo Formations, northern Arizona: eolian-fluvial interactions. In: Brookfield, M.E., Ahlbrandt, T.S. (Eds.), Eolian Sediments and Processes, Dev. Sedimentol, 38. Elsevier, Amsterdam, pp. 613–634. https://doi.org/10.1016/S0070-4571(08)70815-X.
Morley, C.K., 1995. Developments in the structural geology of rifts over the last decade and their impact on hydrocarbon exploration. In: Lambiase, J.J. (Ed.), Hydrocarbon Habitat in Rift Basins, 80. Geol. Soc. London Spec. Pub, pp. 1–32. https://doi.org/10.1144/GSL.SP.1995.080.01.01.
Morrisey, L.B., Braddy, S., Dodd, Ch., Higgs, K.T., Williams, B.P.J., 2012. Trace fossils and palaeoenvironments of the Middle Devonian Caherbla Group, Dingle Peninsula, Southwest Ireland. Geol. J. 47, 1–29. https://doi.org/10.1002/gj.1324.
Mountney, N.P., 2006. Periodic accumulation and destruction of aeolian erg sequences: the Cedar Mesa Sandstone, White Canyon, southern Utah. Sedimentology 53, 789–823. https://doi.org/10.1111/j.1365-3091.2006.00793.x.
Mountney, N.P., 2012. A stratigraphic model to account for complexity in aeolian dune and interdune successions. Sedimentology 59, 964–989. https://doi.org/10.1111/j.1365-3091.2011.01287.x.
Mountney, N.P., Howell, J., 2000. Aeolian architecture, bedform climbing and preservation space in the cretaceous Etjo Formation, NW Nambia. Sedimentology 47, 825–849. https://doi.org/10.1046/j.1365-3091.2000.00318.x.
Mountney, N.P., Jagger, A., 2004. Stratigraphic evolution of an aeolian erg margin system: the Permian Cedar Mesa Sandstone, SE Utah, USA. Sedimentology 51, 713–743. https://doi.org/10.1111/j.1365-3091.2004.00646.x.
Mountney, N.P., Russell, A.J., 2004. Sedimentology of aeolian sandsheet deposits in the Askja region of Northeast Iceland. Sed. Geol. 166, 223–244. https://doi.org/10.1016/j.sedgeo.2003.12.007.
Mountney, N.P., Russell, A.J., 2009. Aeolian dune-field development in a water table-controlled system: Skeiðarársandur, Southern Iceland. Sedimentology 56, 2107–2131. https://doi.org/10.1111/j.1365-3091.2009.01072.x.
Mountney, N.P., Thompson, D.B., 2002. Stratigraphic evolution and preservation of aeolian dune and damp/ wet interdune strata: an example from the Triassic Helsby Sandstone Formation, Cheshire Basin, UK. Sedimentology 49, 805–833. https://doi.org/10.1046/j.1365-3091.2002.00472.x.
Mountney, N.P., Howell, J.A., Flint, S.S., Jerram, D.A., 1999. Climate, sediment supply and tectonics as controls on the deposition and preservation of the aeolian-fluvial Etjo Sandstone Formation, Namibia. J. Geol. Soc. Lond. 156, 771–779. https://doi.org/10.1144/gsjgs.156.4.0771.
Newell, A.J., 2001. Bounding surfaces in a mixed aeolian-fluvial system (Rotliegend, Wessex Basin, SW UK). Mar. Pet. Geol. 18, 339–347. https://doi.org/10.1016/S0264-8172(00)00066-0.
Nielson, J., Kocurek, G., 1986. Climbing zibars of the Algodones. Sed. Geol. 48, 1–15. https://doi.org/10.1016/0037-0738(86)90078-3.
Nield, J.M., Wiggs, G.F.S., Baddock, M.C., Hipondoka, M.H.T., 2017. Coupling leeside grainfall to avalanche characteristics in aeolian dune dynamics. Geology 45, 271–274. https://doi.org/10.1130/G38800.1.
Olsen, H., Larsen, P.-H., 1993. Lithostratigraphy of the continental Devonian sediments in North-East Greenland. Geol. Surv. Denm. Greenl. 165, 1–108. https://doi.org/10.34194/bullggu.v165.6721.
Olsen, H., Due, P.H., Clemmensen, L.B., 1989. Morphology and genesis of asymmetric adhesion warts – a new adhesion surface structure. Sed. Geol. 61, 277–285. https://doi.org/10.1016/0037-0738(89)90062-6.
Paola, C., Borgman, L., 1991. Reconstructing random topography from preserved stratification. Sedimentology 38, 553–565. https://doi.org/10.1111/j.1365-3091.1991.tb01008.x.
Petry, K., Jerram, D.A., de Almeida, D., De, P.M., Zerfass, H., 2007. Volcanic-sedimentary features in the Serra Geral Fm., Paraná Basin, southern Brazil: examples of dynamic lava-sediment interactions in an arid setting. J. Volcanol. Geoth. Res. 159, 313–325. https://doi.org/10.1016/j.jvolgeores.2006.06.017.
Rosendahl, B.R., 1987. Architecture of continental rifts with special reference to East Africa. Ann. Rev. Ear. Plan. Sci. 15, 445–503. https://doi.org/10.1146/annurev.ea.15.050187.002305.
Rubin, D.M., 1987. Cross-bedding, bedforms and palaeocurrents. SEPM Concepts Sed. Paleon. 1, 187. https://doi.org/10.2110/csp.87.01.
Rubin, D.M., Hunter, R.E., 1982. Migration directions of primary and superimposed dunes inferred from compound crossbedding in the Navajo Sandstone. In: Nriagu, J. O., Troost, R. (Eds.), 11th International Congress on Sedimentology, Hamilton, Ontario, August 1982. Int. Assoc. Sedimentol, pp. 69–70.
Ruz, M.-H., Allard, M., 1994. Coastal dune development in cold-climate environments. Phys. Geog. 15, 372–380. https://doi.org/10.1080/02723646.1994.10642523.
Paim, P.S.G., Scherer, C.M.S., 2007. High-resolution stratigraphy and depositional model of wind- and water-laid deposits in the Ordovician Guaritas Rift (southernmost Brazil). Sed. Geol. 202, 776–795. https://doi.org/10.1016/j.sedgeo.2007.09.003.
Pike, J.D., Sweet, D.E., 2018. Environmental drivers of cyclicity recorded in lower Permian eolian strata, Manitou Springs, western United States. Palaeogeog., Palaeoclim. Palaeoecol. 499, 1–12. https://doi.org/10.1016/j.palaeo.2018.03.026.
Porter, M.L., 1986. Sedimentary record of erg migration. Geology 14, 497–500. https://doi.org/10.1130/0091-7613(1986)14<497:SROEM>2.0.CO;2.
Prijac, C., Doin, M.P., Gaulier, J.M., Guillocheau, F., 2000. Subsidence of the Paris Basin and its bearing on the late Variscan lithosphere evolution: a comparison between plate and CHABLIS models. Tectonophysics 323, 1–38. https://doi.org/10.1016/S0040-1951(00)00100-1.
Pulvertaft, T.C.R., 1985. Eolian dune and wet interdune sedimentation in the Middle Proterozoic Dala Sandstone, Sweden. Sed. Geol. 44, 93–111. https://doi.org/10.1016/0037-0738(85)90034-X.
Purser, B.H., Evans, G., 1973. Regional sedimentation along the Trucial Coast, Persian Gulf. In: Purser, B.H. (Ed.), The Persian Gulf. Springer, Berlin, pp. 211–231. https://doi.org/10.1007/978-3-642-65545-6_13.
Pye, K., Tsoar, H., 1990. In: Aeolian Sand and Sand Dunes. Unwin Hyman Limited, London, p. 396.
Pye, K., Tsoar, H., 2008. In: Aeolian Sand and sand Dunes. Springer, p. 138.

Reis, A.D.D., Scherer, C.M.S., Owen, A., Amarante, F.B.D., Ferronatto, J.P.F., Pantopoulos, G., de Souza, E.G., Bállico, M.B., Aguilar, C.A.G., 2022. A quantitative depositional model of a large distributive fluvial system (Megafan) with terminal aeolian interaction: The Upper Jurassic Guará DFS in southwestern Gondwana. J. Sed. Res. 92, 460–485. https://doi.org/10.2110/jsr.2021.040.

Rodríguez-López, J.P., Clemmensen, L.B., Lancaster, N., Mountney, N.P., Veiga, G.D., 2014. Archean to recent aeolian sand systems and their sedimentary record: current understanding and future prospects. Sedimentology 61, 1487–1534. https://doi.org/10.1111/sed.12123.

Romain, H.G., Mountney, N.P., 2014. Reconstruction of 3D eolian-dune architecture from 1D core data through adoption of analogue data from outcrop. AAPG Bull. 98, 1–22. https://doi.org/10.1306/05201312109Ruz.

Sadler, P.M., 1981. Sediment accumulation rates and the completeness of stratigraphic sections. J. Geol. 89, 569–584. https://www.jstor.org/stable/30062397.

Santos, M.G.M., Mountney, N.P., Peakall, J., 2017. Tectonic and environmental controls on Palaeozoic fluvial environments: Reassessing the impacts of early land plants on sedimentation. J. Geol. Soc. 174, 393–404. https://doi.org/10.1144/jgs2016-063.

Santos, M.G.M., Hartley, A.J., Mountney, N.P., Peakall, J., Owen, A., Merino, E.R., Assine, M.L., 2019. Meandering rivers in modern desert basins: Implications for channel planform controls and prevegetation rivers. Sed. Geol. 385, 1–14. https://doi.org/10.1016/j.sedgeo.2019.03.011.

Shaw, R.D., Etheridge, M.A., Lambeck, K., 1991. Development of the late Proterozoic to Mid-Paleozoic, intracratonic Amadeus Basin in Central Australia: a key to understanding tectonic forces in plate interiors. Tectonics 10, 688–721. https://doi.org/10.1029/90TC02417.

Schenk, C.J., Schmoker, J.W., Fox, J.E., 1993. Sedimentology of Permian upper part of the Minnelusa Formation, eastern Powder River Basin, Wyoming, and a comparison to the subsurface. Mount. Geol. 30, 71–80. https://pubs.er.usgs.gov/publication/70017750.

Scherer, C.M.S., 2002. Preservation of aeolian genetic units by lava flows in the lower cretaceous of the Parana Basin, southern Brazil. Sedimentology 49, 97–116. https://doi.org/10.1046/j.1365-3091.2002.00434.x.

Scherer, C.M.A., Lavina, L.C., 2005. Sedimentary cycles and facies architecture of aeolian–fluvial strata of the Upper Jurassic Guara Formation, southern Brazil. Sedimentology 52, 1323–1341. https://doi.org/10.1111/j.1365-3091.2005.00746.x.

Scherer, M.S., Lavina, E.L.C., Dias Filho, D.C., Oliveira, F.M., Bongiolo, D.E., Aguiar, E.S., 2007. Stratigraphy and facies architecture of the fluvial-aeolian-lacustrine Sergi Formation (Upper Jurassic), Reconcavo Basin, Brazil. Sed. Geol. 194, 169–193. https://doi.org/10.1016/j.sedgeo.2006.06.002.

Schlische, R.W., 1993. Anatomy and evolution of the Triassic-Jurassic continental rift system, eastern North America. Tectonics 12, 1026–1042. https://doi.org/10.1029/93TC01062.

Schokker, J., Koster, E.A., 2004. Sedimentology and facies distribution of Pleistocene cold-climate aeolian and fluvial deposits in the Roer Valley graben (Southeastern Netherlands). Perma. Peri. Proc. 15, 1–20. https://doi.org/10.1002/ppp.477.

Scotti, A.A., Veiga, G.D., 2019. Sedimentary architecture of an ancient linear megadune (Barremian, Neuquén Basin): Insights into the long-term development and evolution of aeolian linear bedforms. Sedimentology 66, 2191–2213. https://doi.org/10.1111/sed.12597.

Selley, R.C., Sonnenberg, S.A., 2015. Sedimentary Basins and Petroleum Systems. In: Selley, R.C., Sonnenberg, S.A. (Eds.), Elements of Petroleum Geology, Third Edition. Academic Press, pp. 377–426. https://doi.org/10.1016/B978-0-12-386031-6.00008-4.

Simplicio, F., Basilici, G., 2015. Unusual thick eolian sand sheet sedimentary succession: Paleoproterozoic Bandeirinha Formation, Minas Gerais, Brazil. J. Geol. 45, 3–11. https://doi.org/10.1590/2317-4889201530133.

Simpson, E.L., Eriksson, K.A., 1993. Thin eolianites interbedded within a fluvial and marine succession: Early Proterozoic Whitworth Formation, Mount Isa Inlier, Australia. Sed. Geol. 87, 39–62. https://doi.org/10.1016/0037-0738(93)90035-4.

Sing, P., Kumar, N., 1997. Effect of orography on precipitation in the western Himalayan region. J. Hydrol. 199, 183–206. https://doi.org/10.1016/S0022-1694(96)03222-2.

Sloss, L.L., 1988. Sedimentary cover: North American craton. In: Sloss, L.L. (Ed.), The Geology of North America. Geol. Soc. Am, pp. 1–5. https://doi.org/10.1130/DNAG-GNA-D2.

Sloss, L.L., Speed, R.C., 1974. Relationship of cratonic and continental margin tectonic episodes. In: Dickinson, W.R. (Ed.), Tectonics and Sedimentation, 22. SEPM Spec. Pub, pp. 38–55. https://doi.org/10.2110/pec.74.22.0098.

Sorby, H.C., 1859. On the structures produced by the currents present during the deposition of stratified rocks. The Geol. 2, 137–147. https://doi.org/10.1017/S1359465600021122.

Stel, H., Cloetingh, S., Heeremans, M., van der Beek, P., 1993. Anorogenic granites, magmatic underplating and the origin of intracratonic basins in a non-extensional setting. Tectonophysics 226, 285–299. https://doi.org/10.1016/0040-1951(93)90123-2.

Stewart, J.H., 2005. Eolian deposits in the Neoproterozoic Big Bear Group, San Bernardino Mountains, California, USA. Ear. Sci. Rev. 72, 47–62. https://doi.org/10.1016/j.earscirev.2005.07.012.

Taylor, I.E., Middleton, G.V., 1990. Aeolian sandstone in the Copper Harbor Formation, late Proterozoic, Lake Superior basin. Can. J. Ear. Sci. 27, 1339–1347. https://doi.org/10.1139/e90-144.

Tirsgaard, H., Oxnevad, I.E.I., 1998. Preservation of pre-vegetational mixed fluvio-aeolian deposits in a humid climatic setting: an example from the Middle Proterozoic Eriksfjord Formation, Southwest Greenland. Sed. Geol. 120, 295–317. https://doi.org/10.1016/S0037-0738(98)00037-2.

Trewin, N.H., 1993. Controls on fluvial deposition in mixed fluvial and aeolian facies within the Tumblagooda Sandstone (Late Silurian) of Western-Australia. Sed. Geol. 85, 387–400. https://doi.org/10.1016/0037-0738(93)90094-L.

Wakefield, O.J.W., Mountney, N.P., 2013. Stratigraphic architecture of back-filled incised-valley systems: Pennsylvanian-Permian lower Cutler beds, Utah, USA. Sed. Geol. 298, 1–16. https://doi.org/10.1016/j.sedgeo.2013.10.002.

Werner, B.T., 1995. Eolian dunes: Computer simulations and attractor interpretation. Geology 23, 1107–1110.

Wilson, I.G., 1973. Ergs. Sed. Geol. 10, 77–106. https://doi.org/10.1016/0037-0738(73)90001-8.

Withjack, M.O., Schlische, R.W., Olsen, P.E., 2002. Rift-basin structure and its influence on sedimentary systems. In: Renaut, R.W., Ashley, G.M. (Eds.), Sedimentation in Continental Rifts, 73. Soc. Sed. Geol. Spec. Pub, pp. 57–81. https://doi.org/10.2110/pec.02.73.

Woodcock, N.H., 2004. Life span and fate of basins. Geology 32, 685–688. https://doi.org/10.1130/G20598.1.

Xie, X., Heller, P.L., 2009. Plate tectonics and basin subsidence history. Bull. Geol. Soc. Am. 121, 55–64. https://doi.org/10.1130/B26398.1.

Zang, W.L., 1995. Early Neoproterozoic sequence stratigraphy and acritarch biostratigraphy, eastern Officer Basin, South Australia. Precam. Res. 74, 119–175. https://doi.org/10.1016/0301-9268(95)00007-R.

Zavala, C., Freije, R.H., 2001. On the understanding of aeolian sequence stratigraphy: An example from Miocene-Pliocene deposits in Patagonia, Argentina. Rivis. Ital. Paleont. Stratig. 107, 251–264. https://doi.org/10.13130/2039-4942/5435.